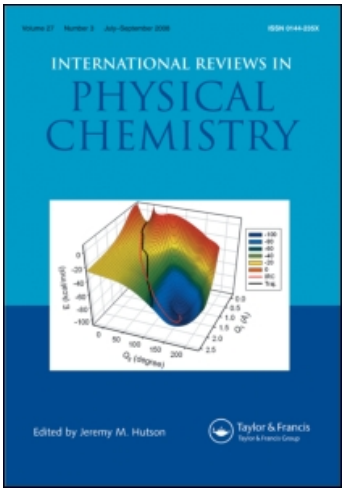

International Reviews in Physical Chemistry
Publication details, including instructions for authors and subscription information:
http://www.informaworld.com/smpp/title~content=t713724383

Paradigm pre-reactive van der Waals complexes: X-HX and X-H_2 (X = F, Cl, Br)

Jacek Klos[a]; M. M. Szczesniak[a]; G. Chalasinski[b]
[a] Department of Chemistry, Oakland University, Rochester, MI 48309, USA [b] Faculty of Chemistry, University of Warsaw, 02-093 Warsaw, Poland

To cite this Article Klos, Jacek , Szczesniak, M. M. and Chalasinski, G.(2004) 'Paradigm pre-reactive van der Waals complexes: X-HX and X-H_2 (X = F, Cl, Br)', International Reviews in Physical Chemistry, 23: 4, 541 — 571
To link to this Article: DOI: 10.1080/01442350500063634
URL: http://dx.doi.org/10.1080/01442350500063634

INT. REVIEWS IN PHYSICAL CHEMISTRY, 2004
VOL. 23, NO. 4, 541–571

Taylor & Francis
Taylor & Francis Group

Paradigm pre-reactive van der Waals complexes: X–HX and X–H_2 (X = F, Cl, Br)

JACEK KLOS†, M. M. SZCZESNIAK† and G. CHALASINSKI‡*

†Department of Chemistry, Oakland University, Rochester, MI 48309, USA
‡Faculty of Chemistry, University of Warsaw, ul. Pasteura 1, 02-093 Warsaw, Poland, and Department of Chemistry, Oakland University, Rochester, MI 48309, USA

(*Received 28 September 2004; in final form 31 December 2004*)

This review describes recent progress in *ab initio* calculations and modeling of weak pre-reactive van der Waals complexes that appear in the entrance channels of benchmark atom–diatom reactions. Examples from recent work are used to demonstrate how relevant potential energy surfaces are obtained and modeled from first principles. The paradigm complexes include the X(^{2}P)–HX and X(^{2}P)–H_2 (X = F, Cl, Br) systems, with O(^{3}P)–HCl included for comparison. In these complexes an interaction with either the HX or the H_2 molecule splits a degenerate P state of an open-shell atom into three potential energy surfaces, two of which are of the same symmetry. Application of state-of-the art highly correlated methods, CCSD(T) and MRCI, to the evaluation of adiabatic and diabatic states is discussed. Nonadiabatic coupling involving potential surfaces is compared for a number of complexes. Computational modeling of this term and its relationship to electrostatic interaction are also described. Spin–orbit coupling is shown to have dramatic effects on the structural and dynamic properties of these complexes.

Contents

*E-mail: dmiller@lphys.chem.utoronto.ca

International Reviews in Physical Chemistry ISSN 0144–235X print/ISSN 1366–591X online
http://www.tandf.co.uk/journals
DOI: 10.1080/01442350500063634

1. Introduction

Open-shell atoms and molecules are very interesting but relatively poorly understood chemical species. Their chemical reactions and inelastic processes make them of key importance in the chemistry of atmospheres, plasmas, lasers and, more recently, ultracold matter. Reactions involving open-shell moieties, especially with nonzero angular momentum, can proceed on multiple potential energy surfaces (PESs) [1]. The presence of electronic nonzero angular momentum induces a new type of electronic anisotropy that leads to the description of intermolecular forces in terms of manifolds of PESs [1]. This electronic anisotropy, as defined by Aquilanti and Grossi [2], is further complicated by additional sources of the angular momentum in these systems [3]. These include angular momenta due to the spin, monomer rotations, and the rotations of the complex as a whole. Spin–orbit coupling leads to additional splitting into an even larger manifold of surfaces. Open-shell reactants also open up reactive channels on the PESs, which further affect their shapes and their mutual interactions.

The outcome of chemical reactions is also profoundly affected by the remote regions of the potential surface, which are governed by long-range forces. These forces have a capacity for orienting the reactants favorably or unfavorably as they approach one another, or may trap them in potential wells before they have a chance to engage in reactive encounters. Dubernet and Hutson [4] state that: ''For any reaction, unless reaction occurs without a potential barrier, there is a minimum on the potential energy surface that can support bound or quasibound van der Waals states.'' There is now a clear consensus that these complexes play a crucial role in determining the course and outcome of chemical reactions. For example, Skouteris *et al.* [5] made a stunning claim that, in the $Cl(^2P) + HD$ reaction, the presence of a tiny van der Waals well (of *ca.* 0.5 kcal/mol) in the entrance valley ahead of a 8.5 kcal/mol barrier strongly affects the distribution of products. They state unequivocally that: ''The study of chemical reaction dynamics has now advanced to the stage where even comparatively weak van der Waals interactions can no longer be neglected in calculations of potential energy surfaces of chemical reactions.'' The pre-reactive van der Waals complex $O(^3P)$–HCl has been implicated in prominent low-energy resonances for this reaction [6]. Many other phenomena, including nonadiabatic processes, are thought to be related to these complexes and to the bound and quasi-bound states they support [7, 8].

Open-shell complexes trapped in such potential wells are very challenging targets for spectroscopic investigations. Energy levels in these complexes are often accessed upon laser excitation of electronic transitions in the complex with methods such as laser-induced fluorescence, resonantly enhanced multiphoton ionization, IR–UV double-resonance fluorescence enhancement, stimulated emission pumping, etc. [9–12]. These techniques have achieved sufficient resolution to provide information about the inter- and intramolecular level patterns of the complex. The ongoing promise of these studies is that this information can be used to gain control over a chemical reaction [13]. One way to induce the reaction within the pre-reactive complex would be to selectively excite the vibrational states of monomers [14]. The other, as postulated by Anderson *et al.* [15], would be to excite the intermolecular modes of vibration so that the complex can sample the configurations that are close to the transition-state structure for the reaction. Spectroscopic studies of these systems could also address a host of other questions that are specific to open-shell systems, such as the splitting of the intermolecular potentials due to the partially filled orbitals, as revealed through Renner–Teller interactions or the rate of spin–orbit relaxation. The quest to obtain these species has intensified in recent years. In favorable circumstances, a neutral open-shell complex can be produced in photoelectron (PE) spectroscopy experiments involving relevant negative ion complexes. Neumark and coworkers carried out such experiments involving $F^-\cdots H_2$ and, more recently, $Cl^-\cdots H_2$ anion complexes. In the case of the former, the photodetachment process accessed the transition state of the $F + H_2$ reaction [16]. In the case of the latter, this process accessed the spin–orbit states of the pre-reactive van der Waals complex $Cl + H_2$ in its reactant valley [17].

Other pre-reactive complexes have also been produced. Wittig's group has generated the Cl–HCl entrance-channel complex by a bond-specific photodissociation of the $(HCl)_2$ complex. The free HCl bond in the complex was first excited by an IR laser and next photodissociated by a UV laser [12]. Che *et al.* [18] have generated its deuterated analog, Cl–DCl, in the photodissociation of a field-selected $(DCl)_2$. A related complex, Br–HF, has recently been produced in helium droplets by Miller's group. They also succeeded in observing an infrared spectrum of the HF stretching region [19].

The availability of sufficiently accurate potential surfaces for the reactive processes has been a crucial factor in advances in experiment and theory. The consensus today is that these calculations should involve highly correlated multireference approaches using very large orbital basis sets [20]. The development of sets of *ab initio* surfaces for the reactive system $F + H_2 \rightarrow FH + H$ by Stark and Werner [21] and for $Cl + H_2 \rightarrow ClH + H$ by Capecchi and Werner [22] from state-of-the-art multireference configuration interaction calculations has been invaluable to both theory and experiment [7, 23–25], including the first unambiguous evidence of Feshbach resonance in the $F + H_2$ reaction [25]. A number of other elementary reactions have recently been described by *ab initio*-generated sets of fully reactive PESs (see Refs [26–30]), which proved to be very useful in quantum reaction dynamics studies [31–33] (see Ref. [34] for a recent comprehensive review).

A common theme in deriving these global surfaces is the "one-size fits all" approach that applies the same treatment to the barriers as to the regions where the long-range forces operate. For example, in the far regions of the $Cl + H_2$ approach, the three adiabats describing this interaction are nearly degenerate. In such circumstances even the MRCI + Q method and its variants may be difficult to apply.

Clearly, the approaches rooted in long-range theory [35–38] can offer useful insights in this area. These van der Waals regions of the reactions can then be attached smoothly to the reactive surfaces, as demonstrated by Dobbyn *et al*. [27].

The first treatment that used the long-range concepts for a description of the pre-reactive region was the semiempirical model approach of Dubernet and Hutson [4, 39]. To build the $Cl(^2P) + HCl$ interaction potentials, they extracted the anisotropy of HCl from the Ar–HCl semiempirical potential and the anisotropy of Cl from Ar–Cl and added the electrostatic terms due to the quadrupole–dipole and quadrupole–quadrupole interactions [39]. Upon including the effects of spin–orbit coupling, they carried out bound state calculations.

In our work we have followed a similar method of characterizing forces in the pre-reactive region by the examination of multiple *interaction* potentials. These potential surfaces and their couplings have been obtained from state-of-the-art *ab initio* calculations for several prototype weak open-shell van der Waals complexes appearing in the entrance channels of benchmark atom–diatom reactions. The halogen atom + molecule complexes studied by our group are $X(^2P)$–HX and $X(^2P)$–H_2 (X = F, Cl, Br), with $O(^3P)$–HCl included for comparison. This review describes recent progress in these calculations and insights gained from these studies.

2. Methods

2.1. *Coordinate system and symmetry*

Complexes of an atom and a linear molecule are described in Jacobi coordinates. The intermolecular vector from the center of mass of the molecule to the atom is denoted **R** and the intramolecular vector is **r**. The angle between the unit vectors of **R** and **r** is denoted Θ (figure 1).

The interaction between the ground-state halogen atom $X(^2P)$ and a molecule removes the degeneracy of the ^2P atomic term (figure 1); the term breaks either into Σ and π states (in the collinear $C_{\infty v}$-symmetry case) or into two states of A′ symmetry and one state of A″ symmetry (in the general C_s-symmetry case), depending on the orientation of the singly occupied p orbital of a halogen atom

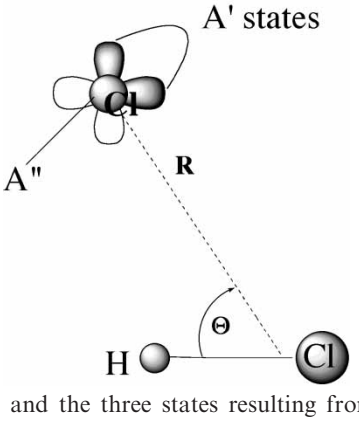

Figure 1. Coordinate system and the three states resulting from the splitting of an atomic term in open-shell atom by the interaction with a linear molecule. The 1A′ and 2A′ states are when the singly-occupied orbital is in the triatomic plane. The A″ is when the singly-occupied orbital is perpendicular to the triatomic plane.

with respect to the triatomic plane. This pattern is identical for $X(^2P) + H_2$, for the collinear and bent C_s arrangements, respectively. In addition, for the T-shape geometries, which are of C_{2v} symmetry, 1A′, 1A″ and 2A′ correlate to A_1, B_1 and B_2 states, respectively. By contrast, the $O(^3P)$ atom has one doubly-occupied and two singly-occupied 2p orbitals. Consequently, in an interaction with HCl, there are two states of A″ symmetry and one of A′ (in the C_s geometry case).

The key ingredients of any approach should include: (i) adiabatic potential energy surfaces calculations, (ii) a transformation to a diabatic representation, and (iii) a procedure to account for spin–orbit coupling. All elements of this methodology were outlined previously [40] (see also [41] for an excellent introduction to this field).

2.2. *Computational approaches*

In *ab initio* calculations of coupled PESs, it is customary to use multireference methods based on a complete active space self-consistent field (CASSCF) model, followed by a multireference configuration interaction (MRCI) treatment [42]. Unfortunately, in the context of weak van der Waals complexes, extracting interaction energies from the MRCI supermolecular (dimer) calculations is far from trivial. The use of the supermolecular approach is complicated by the fact that MRCI is not size-extensive. Approximate size-consistency corrections, although relatively accurate with respect to total energies, are insufficiently accurate with respect to (several orders of magnitude smaller) interaction energies. To circumvent this problem the MRCI dimer calculations customarily refer to the asymptotic limit obtained from a dimer calculation at some artificially large separation, rather than to two separately calculated monomer energies. However, such an approach hinders the application of counterpoise corrections, which require the calculations of monomer energies within the basis set of the whole dimer [43]. Within the MRCI framework the separate monomers cannot be defined in a consistent manner. There are other weaknesses of MRCI as well. First, this is the most time- and memory-intensive of all *ab initio* methods. Second, the method requires several arbitrary choices, such as, for example, a partitioning into inactive, active and secondary orbitals, which make it impossible to design a sequence of convergent calculations with respect to the one-electron basis set and model space extensions. Third, although multireference configuration interaction singles and doubles (MRCISD) accounts selectively for more than double excitations, the intermonomer triple and higher excitations that are essential for the dispersion interaction are not included. Our results indicate [44] that, because of the absence of triple excitations, the dispersion energy may be underestimated by as much as 30%!

The most accurate approach is an open-shell single-reference coupled-cluster treatment with single, double and noniterative triple excitations and applied in the partially spin-restricted [RCCSD(T)] framework. This approach is size-extensive and, because of the inclusion of triple excitations, highly accurate in treating the dispersion-bound complexes. It is, however, limited to the instances where the Hartree–Fock determinant represents a reasonable first approximation.

An optimal *ab initio* method should combine the multireference framework with the coupled-cluster ansatz (MR-CC). The development of such multireference, multiroot, as well as state-selective (single-root), schemes has intensified in recent years (see Ref. [45] for a recent overview). Some new implementations have recently been tested in the context of a challenging weakly-bound open-shell system

$(NO)_2$ [46]. It is not yet clear whether these approaches will be applicable in the context of weak van der Waals interactions with the counterpoise (CP) correction.

2.3. *Transformation to diabatic basis*

The *ab initio* calculations neglecting spin lead to Born–Oppenheimer (adiabatic) states $\{\Psi_i^{\mathrm{a}}\}$ that represent a poor choice for scattering or dynamics calculations. If the scattering problem is solved within the Born–Oppenheimer approximation with intersecting potentials, the electronic (and hence also nuclear) wave functions are not single-valued. As a result, it is difficult to impose boundary conditions. This problem is circumvented in the diabatic representation $\{\Psi_i^{\mathrm{d}}\}$, in which the electronic wave functions are always single-valued. Dynamic calculations require additional information beyond that contained in the adiabatic potentials, such as the nonadiabatic couplings. Diabatic states can be obtained by a unitary transformation of the adiabatic states,

$$\Psi_i^{\mathrm{d}} = \sum_j \Psi_j^{\mathrm{a}} \cdot U_{ji} \tag{1}$$

where U is chosen from the criterion

$$\left\langle \Psi_j^{\mathrm{d}} \middle| \partial/\partial q \middle| \Psi_i^{\mathrm{d}} \right\rangle = 0 \tag{2}$$

for all the coordinates q. In the case of two interacting states of the same symmetry, the transformation U can be determined by the single adiabatic-to-diabatic transformation angle γ [47] (also referred to as the mixing angle):

$$U = \begin{pmatrix} \cos\gamma & \sin\gamma \\ -\sin\gamma & \cos\gamma \end{pmatrix} \tag{3}$$

For a P-state atom the γ angle can be conveniently obtained from the matrix elements of the orbital angular momentum operator [48] between the adiabatic wave functions (see below). An important aspect of diabatization arises from the fact that the interaction of states is represented by a diabatic potential matrix that is not diagonal. This gives rise to extra potential surfaces that are necessary for bound-state and scattering calculations. In a two-state case there is one such potential term (also referred to as the diabatic coupling term) that can be related to the mixing angle γ [41]. The off-diagonal term can often be reliably predicted using some physically sensible model, such as an electrostatic interaction [36, 37, 49]. Our results show (see below) that the *ab initio* and electrostatic models agree remarkably well, not only at large separations but even in the neighborhood of the van der Waals minimum.

2.4. *Spin–orbit coupling*

In the $X(^2P)$–HX and $X(^2P)$–H_2 complexes the X atom is the source of spin–orbit coupling. Let us denote the operators of orbital and spin angular momentum of X as $\boldsymbol{L}$ and $\boldsymbol{S}$, and $\boldsymbol{j}_{\mathbf{a}} = \boldsymbol{L} + \boldsymbol{S}$ the total atomic angular momentum. The atomic splitting of the $^2P_{1/2} - {}^2P_{3/2}$ states for F, Cl and Br are shown in table 1. This splitting is much larger than the anisotropy of the van der Waals interaction and, in such circumstances [4, 39], it is possible to use a coupled atomic basis set $|j_{\mathrm{a}}\omega\rangle$, where j_{a} quantizes the total angular momentum of X and ω its projection onto the $\mathbf{R}$ vector. In this basis set the spin–orbit Hamiltonian $H_{\mathrm{SO}} = A\ \boldsymbol{L}\cdot\boldsymbol{S}$ is diagonal. The spin–orbit

Table 1. Quadrupole moments (a.u.) from CASSCF calculations of Medved *et al.* [50] and experimental Δ_{SO} (cm^{-1}).

Atom	Quadrupole moment	Δ_{SO}
$F(^2P)$	0.726	404.14
$Cl(^2P)$	1.702	882.35
$Br(^2P)$	2.186	3685.24
$O(^3P)$	−1.021	158.26
		226.98

parameter A is assumed to be constant, that is independent of R and in the van der Waals region. For the Cl–HCl complex we report below the results of Zeimen *et al.* [49], who added the SO coupling to our diabatic potentials. We followed the same approach for the remaining X–HX complexes. For F–H_2, Alexander *et al.* described the treatment of the SO coupling in the fully uncoupled basis set of the X atom [23]. We followed this approach for the remaining X–H_2 complexes. For the purposes of discussing ground states of the latter complexes, the total angular momentum of a complex is denoted $\boldsymbol{J}$ and the angular momentum due to the rotation of the H_2 subunit is denoted $\boldsymbol{j}$.

3. Potential energy surfaces for pre-reactive complexes

3.1. *Suitability of single-reference approaches*

It is generally accepted that in open-shell systems the lowest state of a given symmetry can be adequately treated within the single reference approach (unless the nondynamic correlation is important). In favorable circumstances this can also be true of excited states of the same symmetry. Szalay and Gauss demonstrated that an excited state described by a promotion of one electron from a singly occupied orbital to another orthogonal orbital should be amenable to a single-reference treatment, such as the restricted open-shell coupled-cluster method [51]. The interactions $X(^2P) + HX/H_2$ represent such a case as the lowest two states of the A' symmetry differ by the occupation of two p orbitals.

Another enabling factor for the single-reference treatments is the presence of a nonzero quadrupole moment of a ^2P state atom. The ensuing electrostatic interaction is crucial to the separation between the two lowest states of the same symmetry. In the case of $X(^2P) + HX$, the separation of these states is fairly strong due to the substantial quadrupole(X)–dipole(HX) and quadrupole(X)–quadrupole(HX) interactions. In the case of $X(^2P) + H_2$, the adiabatic states are much closer due to quadrupole(X)–quadrupole(H_2) interactions, which are much weaker.

Our group has reported *ab initio* results for two types of such complexes: $Cl(^2P) + HCl$ [52] and $X(^2P) + H_2$ (X–halogen) [53–55]. $Cl(^2P) + HCl$ served as a basis for a detailed comparison between the coupled cluster and MRCI approaches, which demonstrated that the three lowest adiabatic states, 1A′, 2A′ and A″, can be reliably calculated using the restricted open-shell CCSD(T) method for this and the other related $X(^2P) + HX$ complexes. By contrast, for the $X(^2P) + H_2$ complexes we

found that the splitting was too small and an alternative approach, which is discussed in Section 3.3.5, was applied.

3.2. *Counterpoise correction*

In calculations of multiple PESs it is a common practice to calculate PES as total energies without correction for the basis set superposition error (BSSE). Figure 2 shows the consequences of such an approach to the van der Waals region of the Br–HBr complex. The total dimer energies (left panel) of the three lowest adiabatic states are compared with the same three states evaluated as interaction energies and counterpoise corrected (right panel) with the energy scale kept approximately the same. It is seen that both approaches lead to a different splitting among the states, and the appearance of some spurious features on the PESs, such as the inexplicable maximum around $\Theta = 150^\circ$ on the 1A′ adiabat [40].

Calculations of the counterpoise correction for an open-shell moiety are based on the realization that the ghost basis set splits its atomic term into a number of monomer states. The practical calculations of these states require a proper orientation of the singly-occupied orbital with respect to the ghost site. Such calculations can be carried out straightforwardly in most of the electronic structure codes. Achieving a desired orientation of the singly-occupied orbital in the monomer-plus-ghost calculations proved to be more convenient in the diabatic representation (where different states have this orientation fixed with respect to **R**) [41]. In this approach the counterpoise correction is applied to the diabatic PESs and the BSSE-corrected adiabats are obtained upon diagonalization. It is also possible to obtain monomer energies with singly-occupied orbitals pre-oriented exactly as they are in the adiabatic states of the dimer (see Ref. [52] for more details). It is noteworthy that the calculations for the off-diagonal diabatic potential do not require counterpoise correction as the coupling is related to the difference between two *dimer* energies (at the same geometry) rather than between the dimer and the separated monomers.

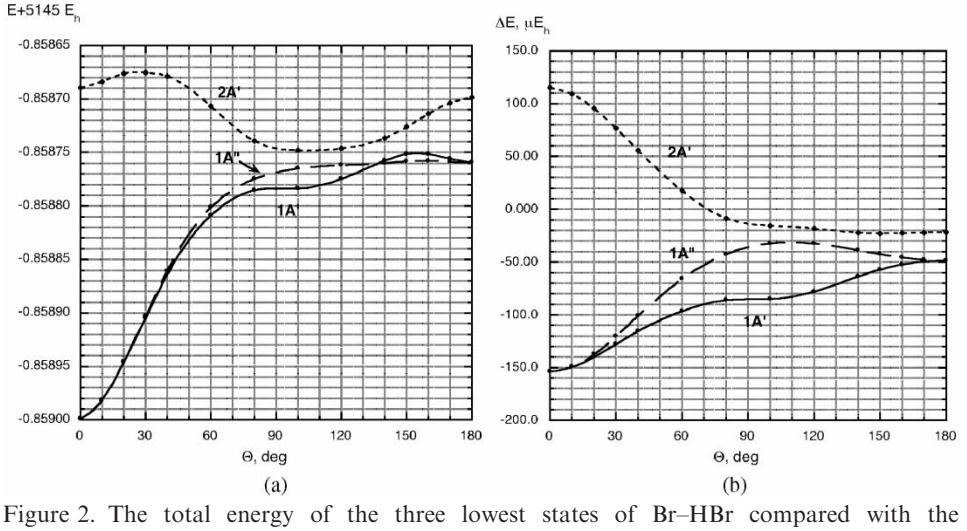

Figure 2. The total energy of the three lowest states of Br–HBr compared with the interaction energies of the same three states from RCCSD(T) calculations (basis set is aug-cc-pvtz + bond functions).

3.3. *Specific details of $X(^2P) + HX$ calculations*

Potential energy surfaces were derived assuming the HX monomers to be rigid. The three adiabatic potentials, 1A′, 2A′ and 1A″, were calculated using the partially restricted CCSD(T) approach. In the simultaneous calculations, the 1A′ and 2A′ states were obtained by the state-averaged CASSCF followed by MRCI. The MRCI states were then used to obtain the mixing angle γ using the following relation

$$\gamma_{\mathrm{LF}} = \arctan \frac{\langle 1\mathrm{A}'|L_i|1\mathrm{A}''\rangle}{\langle 2\mathrm{A}'|L_i|1\mathrm{A}''\rangle} \tag{4}$$

involving an appropriate component of the angular momentum operator. It should be stressed that such transition-moment calculations require neither counterpoise nor size-consistency corrections. The transformation to the diabatic representation provided the following four potential surfaces:

$$\begin{aligned} V_{11} &= V_{1\mathrm{A}'} \cos^2 \gamma_{\mathrm{BF}} + V_{2A'} \sin^2 \gamma_{\mathrm{BF}} \\ V_{22} &= V_{1\mathrm{A}'} \sin^2 \gamma_{\mathrm{BF}} + V_{2\mathrm{A}'} \cos^2 \gamma_{\mathrm{BF}} \\ V_{12} &= (V_{1\mathrm{A}'} - V_{2\mathrm{A}'}) \cos \gamma_{\mathrm{BF}} \sin \gamma_{\mathrm{BF}} \\ V_{33} &= V_{\mathrm{A}''} \end{aligned} \tag{5}$$

where γ_{BF} denotes the mixing angle transformed from the laboratory- (LF) to the body-fixed (BF) coordinate system.

The calculations used extended basis sets of at least aug-cc-pvtz quality. These atom-centered basis sets are still insufficient to saturate the dispersion interaction. The slow convergence of the dispersion energy originates in the Coulomb cusp condition, which is difficult to satisfy by the monomer-centered basis-set expansion. A simple remedy involves the addition of bond functions in the middle of a van der Waals bond [56]. The majority of calculations described here used bond functions. It should be mentioned, however, that bond functions have a tendency to increase BSSE and to alter the electrostatic energy, and for these reasons they should be used with caution [40].

3.3.1. *$Cl(^2P) + HCl$*

The three adiabatic potentials, 1A′, 2A′ and 1A″, calculated for the pre-reactive complex $Cl(^2P) + HCl$ [52] are shown in figure 3. The basis set used in these calculations consisted of aug-cc-pvtz augmented by a set of 3s3p2d bond functions.

The lower of A′ adiabats has the global minimum (600 cm^{-1}) for the T-shaped orientation, and a secondary minimum (440 cm^{-1}) for the hydrogen-bonded configuration. The upper one has a shallow minimum (120 cm^{-1}) for the non-hydrogen-bonded structure. The A″ adiabat has a double-minimum character with one minimum for the hydrogen-bonded (deeper) and one for the non-hydrogen-bonded structure. The effects of adding the SO coupling are very important (see figure 4) on the lower SO adiabat the T minimum became shallower by one-half, while the H-bonded minimum remained the same as on the spin-free adiabat. It is noteworthy that the uppermost SO-adiabat, which correlates with the $^2P_{1/2}$ atomic asymptote, becomes nearly isotropic, retaining the characteristics of the Ar–HCl surface. This is caused by the fact that $Cl(^2P_{1/2})$ has no quadrupole moment (see also Section 3.3.5).

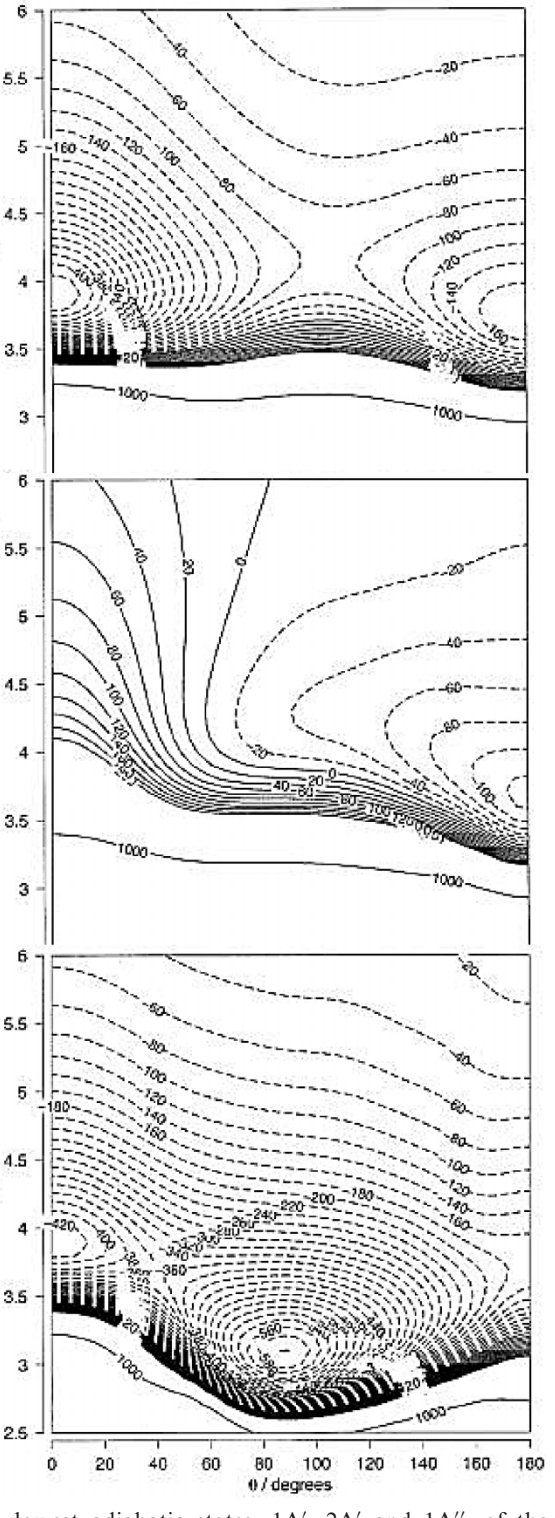

Figure 3. The three lowest adiabatic states, 1A′, 2A′ and 1A″, of the Cl + HCl complex from RCCSD(T) calculations. Energy contours are in cm^{-1}.

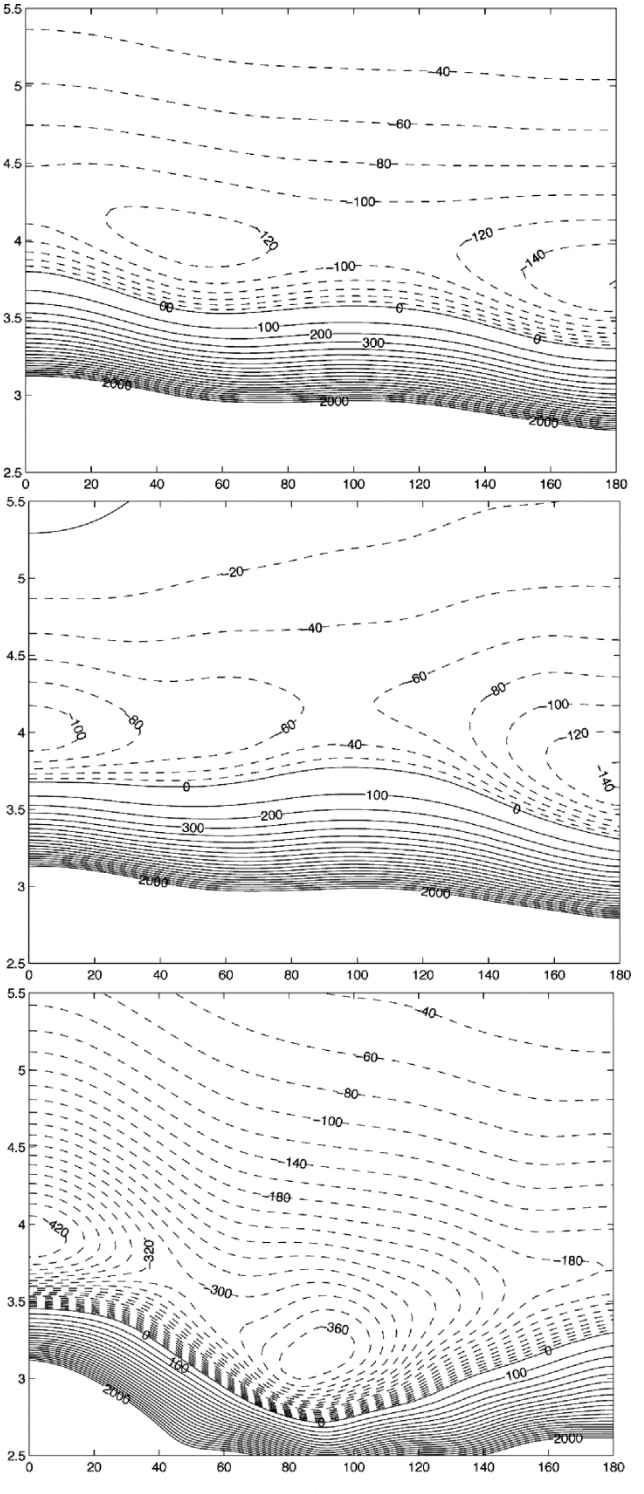

Figure 4. The three lowest adiabatic states of the Cl + HCl complex after inclusion of S–O coupling. The lowest two correlate with the $^2P_{3/2}$ atomic state and the upper one correlates with the $^2P_{1/2}$ state (raised by 882.35 cm^{-1}). Energy contours are in cm^{-1}.

3.3.2. *$F(^2P) + HF$ and $Br(^2P) + HBr$*

The other $X(^2P) + HY$ (where X, Y are halogen) complexes, F + HF [57], Br + HBr [58] and Br + HF [59], have also been studied recently by a variety of methods. For F + HF, Meuwly and Hutson [57] obtained the semiempirical van der Waals PESs by applying the approach that was previously proposed by Dubernet and Hutson for Cl + HCl [39]. Bitterova and Biskupic attempted to characterize the minimum region of F + HF by MRCI [60], and we have performed some preliminary *ab initio* calculations [61] using the RCCSD(T)/aug-cc-pvtz + bf(3s3p2d2f1g) method for the adiabatic potentials and MRCI/aug-cc-pvtz calculations of the mixing angle. For Br + HBr, Meuwly and Hutson applied the semiempirical approach [58] and we have studied this complex with an *ab initio* approach [61]. The RCCSD(T)/aug-cc-pvtz + bf(3s3p2d) treatment of adiabatic surfaces was combined with the MRCI/aug-cc-pvtz calculations of the mixing angle. Our *ab initio* treatment of both F + HF and Br + HBr included SO coupling. For the Br + HF interaction only the semiempirical approach has been applied to date, by Meuwly and Hutson [59].

It is interesting to compare some features of the F + HF, Cl + HCl and Br + HBr complexes. The lowest spin-free $1A'$ PESs of F + HF and Br + HBr are shown in figure 5 (cf. figure 3 for Cl–HCl). The qualitative characteristics of Cl + HCl and Br + HBr are similar, with Br + HBr displaying an even deeper T-shaped minimum than Cl + HCl. The F + HF is qualitatively different, with the linear H-bonded minimum being deeper.

Figure 6 compares the mixing angles for F + HF, Cl + HCl and Br + HBr complexes. It may be recalled at the outset that the extreme angles, 0° and 90°, correspond to zero coupling, that is to pure noninteracting states. The 45° angle corresponds to maximal coupling that results either in degeneracy (conical intersection) or in avoided crossing. Two characteristic features of the mixing angle are notable. First, for all three systems there is a remarkable similarity of the plots in the vicinity of the H-bonded geometries ($\Theta = 0°$). Each system displays a single short-range conical intersection where an avoided crossing originates and continues towards the bent geometries ($\Theta = 60°$) in the asymptotic region. By contrast, in the vicinity of the non-H-bonded geometries ($\Theta = 180°$) there are striking differences between the systems: whereas for F–HF the mixing angle is close to zero, Cl–HCl features a loop of strong coupling that links two conical intersections, short-range and long-range. We show later that the mixing angle for the $O(^3P) + HCl$ complex displays similar characteristics. Br + HBr is different, having only a single short-range intersection (at least within the range of R considered in our calculations). While the existence of the $\Theta = 0°$ crossings (reactive) is well known [62], the appearance of one or two crossings on the nonreactive side, $\Theta = 180°$, in heavier halogens has not been known up to now. It is yet to be determined whether these crossings will "survive" stretching of the H–X bond. Conical intersections are implicated in a variety of electronic nonadiabatic processes [63, 64]. It is interesting to note that the entrance valleys of X + HX complexes are potentially rich grounds for such phenomena.

The role of the SO coupling in the three complexes is shown in figure 7 (for F–HF and Br–HBr) and figure 5 (Cl–HCl). The complexes Cl–HCl and Br–HBr are very strongly and qualitatively affected by the SO coupling in that their T-shaped minima are almost completely washed out and the complexes become linear in their minimum structures. In F + HF, where the halogen's coupling constant is much smaller (see table 1), the linear minimum remains the global one. We conclude that

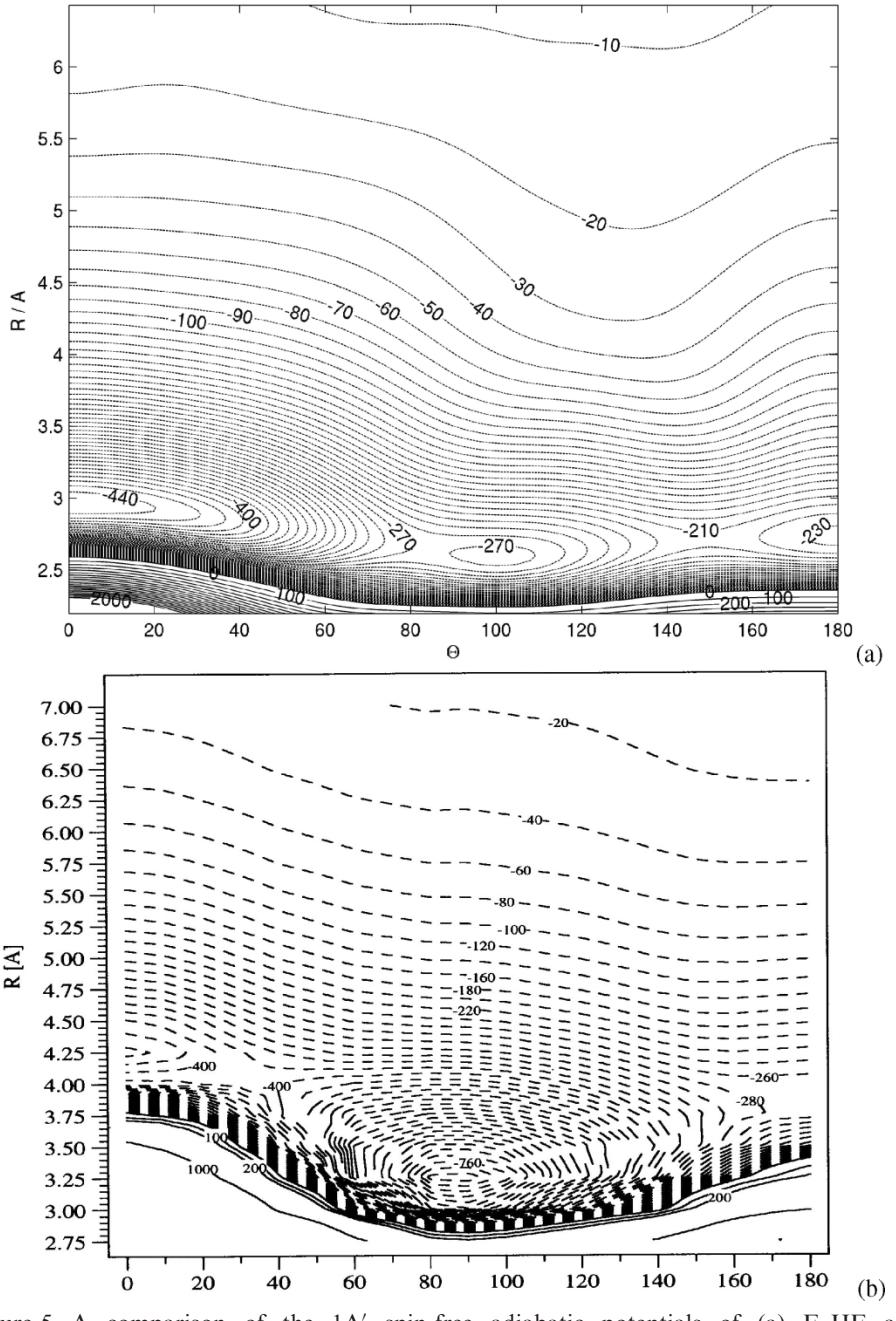

Figure 5. A comparison of the 1A′ spin-free adiabatic potentials of (a) F–HF and (b) Br–HBr (from RCCSD(T) calculations). Energy contours are in cm^{-1}.

the spin-free picture of halogen–radical complexes can be totally misleading: positions of minima (i.e. the equilibrium structures, well depths, etc.) may be misrepresented. The effects of the spin–orbit coupling on the reaction probability in the Cl + HCl reaction was studied previously by Schatz *et al*. [62]. They found that

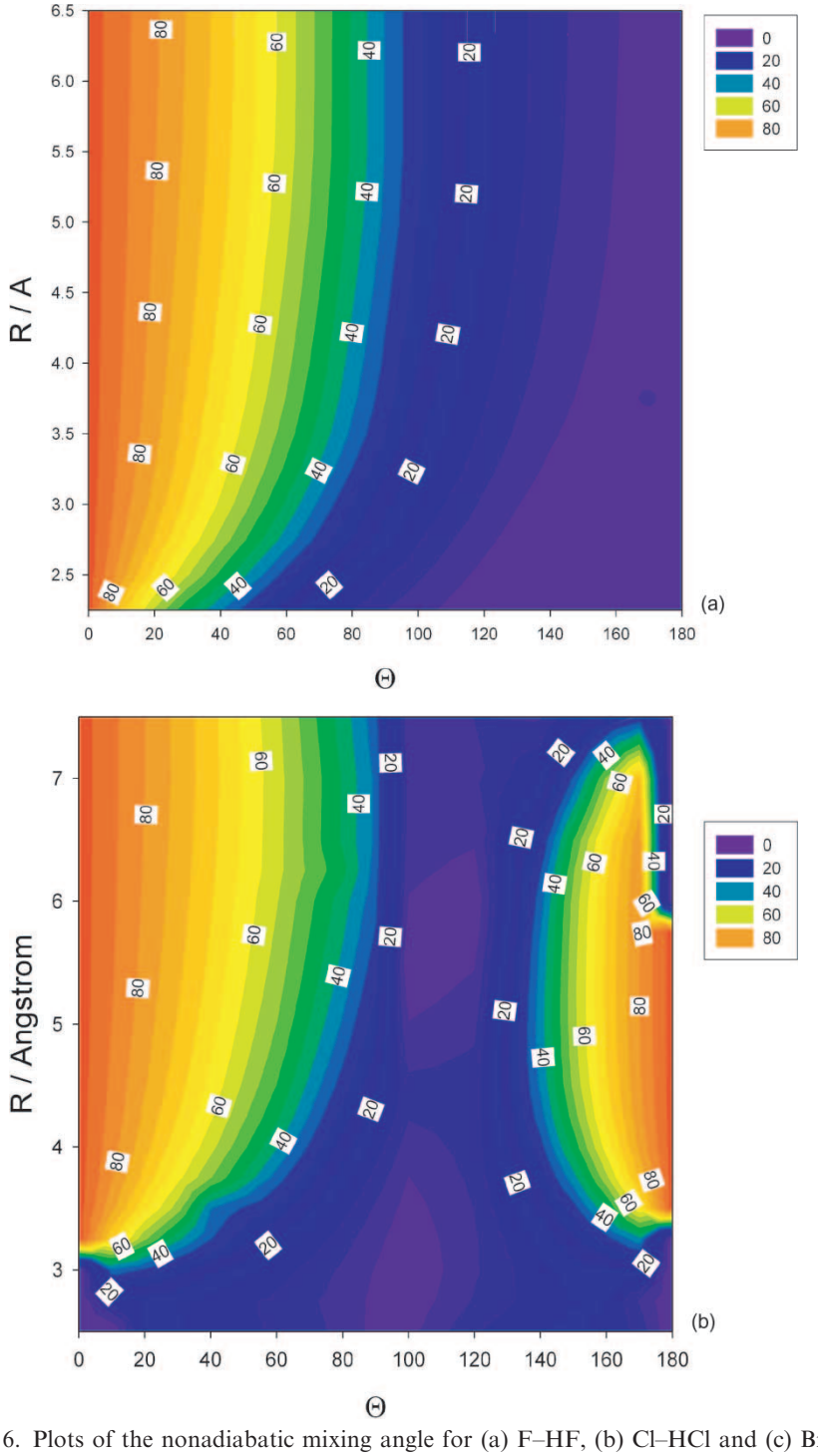

Figure 6. Plots of the nonadiabatic mixing angle for (a) F–HF, (b) Cl–HCl and (c) Br–HBr from MRCI calculations (see equation 2). For Cl–HCl, the sharp feature around $6 < R < 7$ and $150 < \Theta < 175^{\circ}$ is probably an artifact of the calculations.

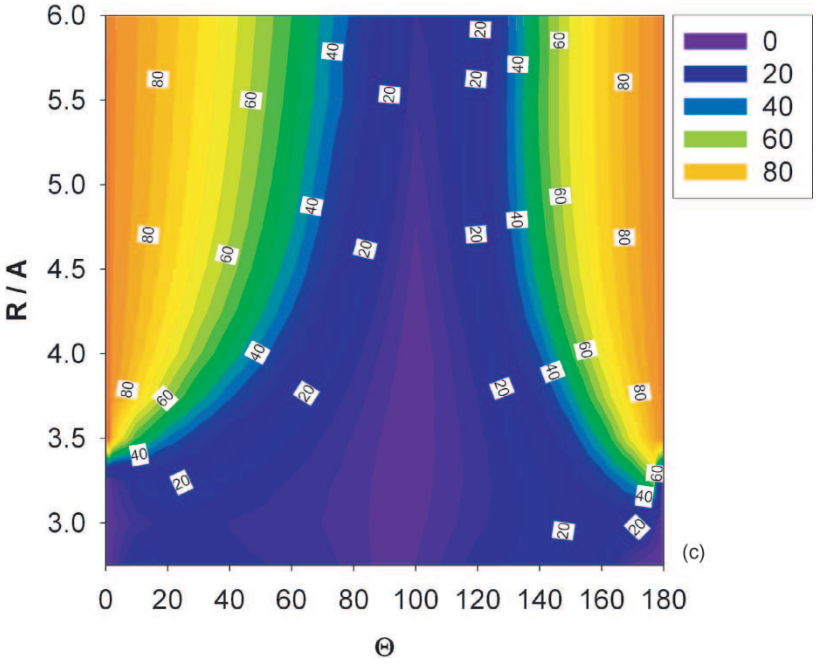

Figure 6. Continued.

the $^2P_{3/2}$ state has higher reactivity, but also predicted that a reversal may occur for atoms with smaller spin–orbit splittings, such as the first-row elements.

In the interaction of halogens that have substantial electron affinities, the role of ion pair states may be important. Figure 8 compares the neutral states of Br–HBr and excited states $Br^- - HBr^+$ of the ion-pair type. The CASSCF calculations of these states computed at $R = 3.175$ Å indicate that the ion-pair states are more strongly bound than the neutral states (as expected) and they are well separated from the lower states.

3.3.3. *Comparison with the semiempirical model of Dubernet and Hutson*

Our *ab initio* PESs can be compared with the semiempirical results for F + HF [57], Cl + HCl [39] and Br + HBr [58] obtained by Hutson and collaborators. The comparison in table 2 involves the ground adiabatic states of the three complexes at three stationary points: the H-bonded ($\Theta = 0°$), T-shaped and non-H-bonded ($\Theta = 180°$) geometries. The upper states are in almost quantitative agreement in both approaches. At the spin-free level, the semiempirical model leads to two nearly equally deep minima (H-bonded and T-shaped) for F + HF and Cl + HCl, whereas for Br–HBr only a single minimum (T-configuration) and a flat region on the non-H-bonded side are found. As discussed above (see figures 3a and 5 and table 2), the *ab initio* calculations reveal a somewhat different picture. The F + HF has a global H-bonded minimum (and traces of the minima for the other two geometries), while both Cl + HCl and Br + HBr have deep global minima for the T-configuration and local ones for the H-bonded geometry. In both approaches, the inclusion of SO-coupling affects primarily the bent configurations. In the semiempirical approach this leads to a flattening of the T minimum in F + HF and its disappearance in

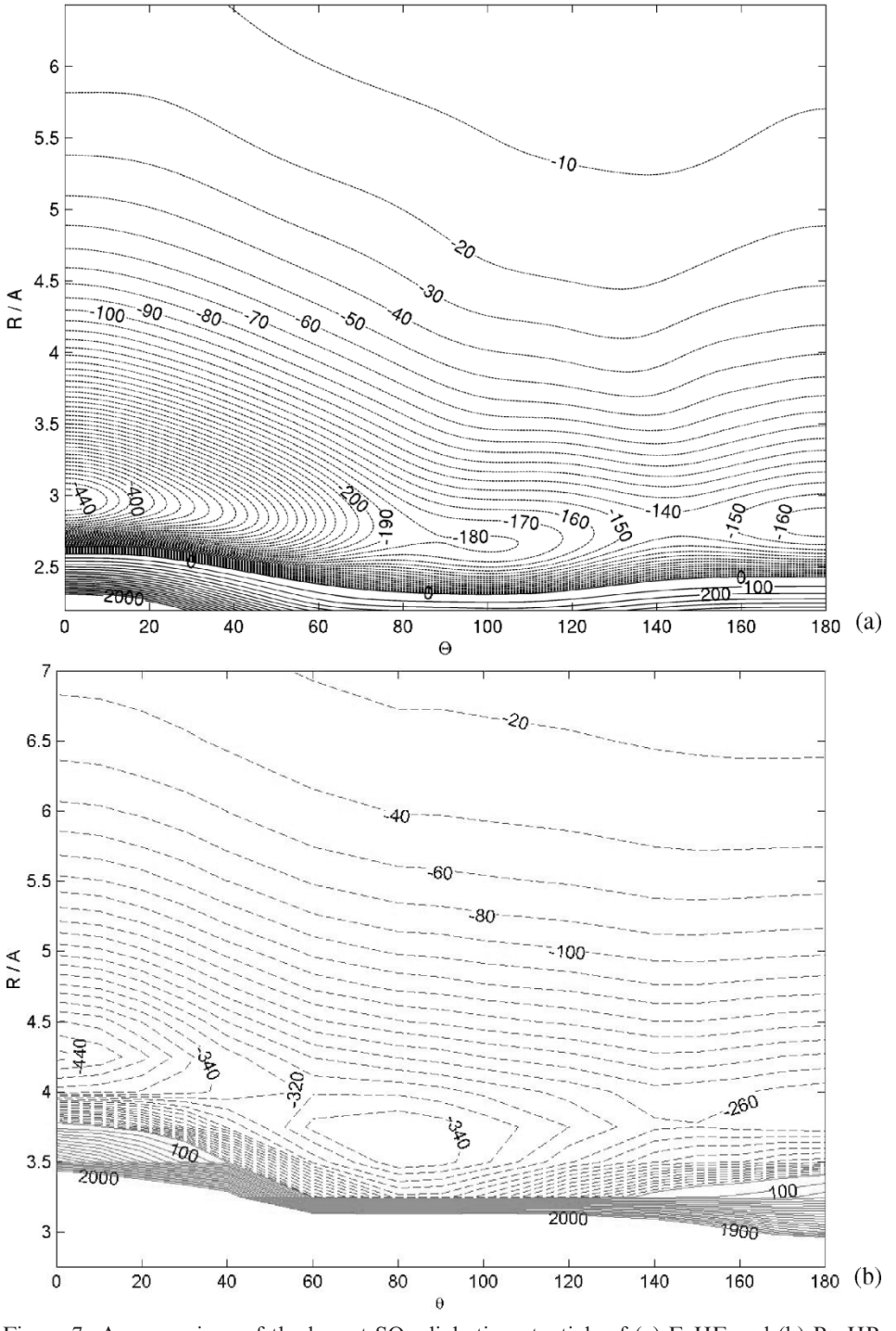

Figure 7. A comparison of the lowest SO-adiabatic potentials of (a) F–HF and (b) Br–HBr (from RCCSD(T) calculations). Energy contours are in cm^{-1}.

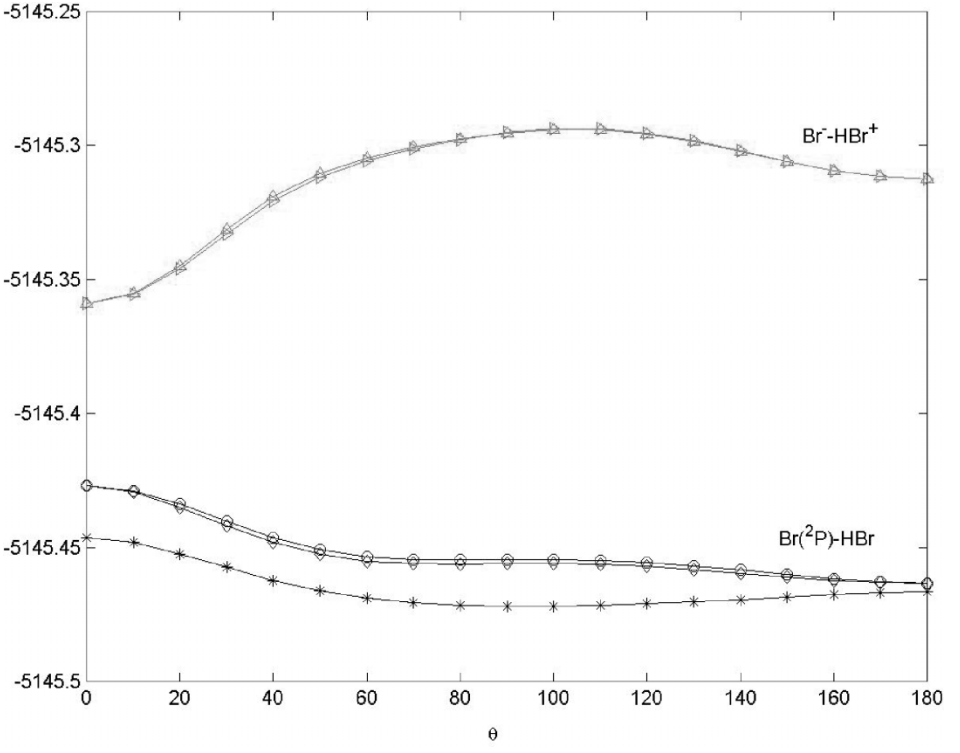

Figure 8. A comparison of the neutral and ion-pair states in Br–HBr from CASSCF calculation at $R = 3.175$ Å; energy units are hartrees.

Table 2. Comparison of *ab initio* [52, 61] characteristics of the lowest spin-free (1A′) and SO (SO-1)-adiabats for the X + HX (X = F, Cl, Br) complexes with the semiempirical model of Hutson and coworkers [39, 57, 58]. The energy values are in cm^{-1}. The energies marked by an asterisk correspond to geometries that are not minima.

Geometry	Method	F + HF		Cl + HCl		Br + HBr	
		1A′	SO-1	1A′	SO-1	1A′	SO-1
H-bonded	*ab initio*	−449	−449	−438	−438	−450	−450
	semiempirical	−317	−317	−383	−383	−342*	−342
T-shaped	*ab initio*	−270	−180	−600	−377	−830	−340
	semiempirical	−280	−200	−347	−240*	−387	−240*
Non-H-bonded	*ab initio*	−230	−165	−180*	−180*	−280	−280
	semiempirical	−110*	−90*	−200*	−200	−307	−307

Cl + HCl and Br + HBr. It also "'carves" the secondary non-H-bonded minima in the latter two complexes. In the *ab initio* case, the T wells in Cl + HCl and Br + HBr are also almost washed out to become shallow secondary minima.

The semiempirical and *ab initio* results reveal many similarities and some differences, which tend to diminish after including the SO coupling. Both approaches predict the global minima to occur at the H-bonded configuration for all three

systems with remarkably similar well depths. The *ab initio* D_e estimates are 449, 438 and 450 cm^{-1} for F + HF, Cl + HCl and Br + HBr, respectively, while the semiempirical values are uniformly smaller (317, 383 and 342 cm^{-1} for F + HF, Cl + HCl and Br + HBr, respectively). The semiempirical results also find F + HF to be qualitatively dissimilar to the other two complexes (see above). This points to the electrostatic nature of this difference (smaller quadrupole moment of F than those of Cl and Br, but larger dipole moment of HF than those of HCl and HBr). The major difference between the two approaches pertains to the depth of the T-shaped minima in the Cl + HCl and Br + HBr complexes. Although these minima nearly disappear when the SO effects are switched on, it is worthwhile speculating on their origin. The semiempirical potentials, by their design, include the dispersion, short-range repulsion and electrostatic-multipole components of the interactions between X and HX, but underestimate the effects due to electric polarization [65]. The inclusion of the latter effects should further stabilize the T-shaped and H-bonded regions.

Overall, the semiempirical model of Dubernet and Hutson [4, 39] works remarkably well for complexes of halogen atoms with hydrogen halides. It provides a deep understanding of the underlying interactions and a very reasonable description of PESs in nearly quantitative agreement with *ab initio* calculations.

3.3.4. $O(^3P) + HCl$

Another pre-reactive complex of great interest is $O(^3P) + HCl$. The full reaction $O + HCl \rightarrow OH + Cl$ has been studied by *ab initio* treatment. Ramachandran and Peterson [66] obtained the two lowest surfaces of $^3A''$ and $^3A'$ symmetry for the whole reaction by applying the MRCI + Q method and a series of relatively large basis sets leading to the "complete basis set" (CBS) extrapolation. Manolopoulos *et al.* [6] observed a number of low-energy resonances in the cumulative reaction probability of this reaction and concluded that they are related to the quasi-bound states due to the entrance-channel van der Waals complexes. A similar *ab initio* methodology to that developed for Cl + HCl [52] was used to compute the three lowest states of the $O(^3P) + HCl$ complex: $1A''$, $2A''$ and $1A'$ (C_s geometry) [67]. Because of the $O(^3P)$ atom's quadrupole moment (see table 1), the $O(^3P)$–HCl interaction has a significant quadrupole(O)–dipole(HCl) and quadrupole(O)–quadrupole(HCl) electrostatic component.

The similarities and contrasts between these complexes can be seen in figure 9. In the H-bonded ($\Theta = 0^\circ$) linear configurations (figure 9a), the O + HCl and Cl + HCl potentials are very similar, although the Σ and π states are reversed. Both complexes have one reactive state crossing at short range (O–HCl at $R = 2.6$ Å and Cl–HCl at $R = 3.1$ Å). In the non-H-bonded linear configuration ($\Theta = 180^\circ$) the potentials intersect twice (figure 9b), at the short and at the long distance. The lowest $1A''$ adiabat has a single minimum for the H-bonded configuration with a well depth of about 580 cm^{-1} (see table 3). The upper $2A''$ adiabat has a single shallow minimum (*ca.* 60 cm^{-1}) on the opposite side. The $1A'$ adiabat has a single minimum for a T-shaped geometry with a well depth of about 120 cm^{-1}. It is interesting to examine the mixing angle for O + HCl (figure 10). The plot is strikingly similar to that for Cl + HCl of figure 7b (except for the reversal of 0° and 90° mixing angles). There is a single conical intersection on the H-bonded side and an avoided crossing that turns towards $\Theta = 60^\circ$ in the asymptotic region. On the non-H-bonded side the avoided crossing forms a loop connecting the two conical intersections. It should be

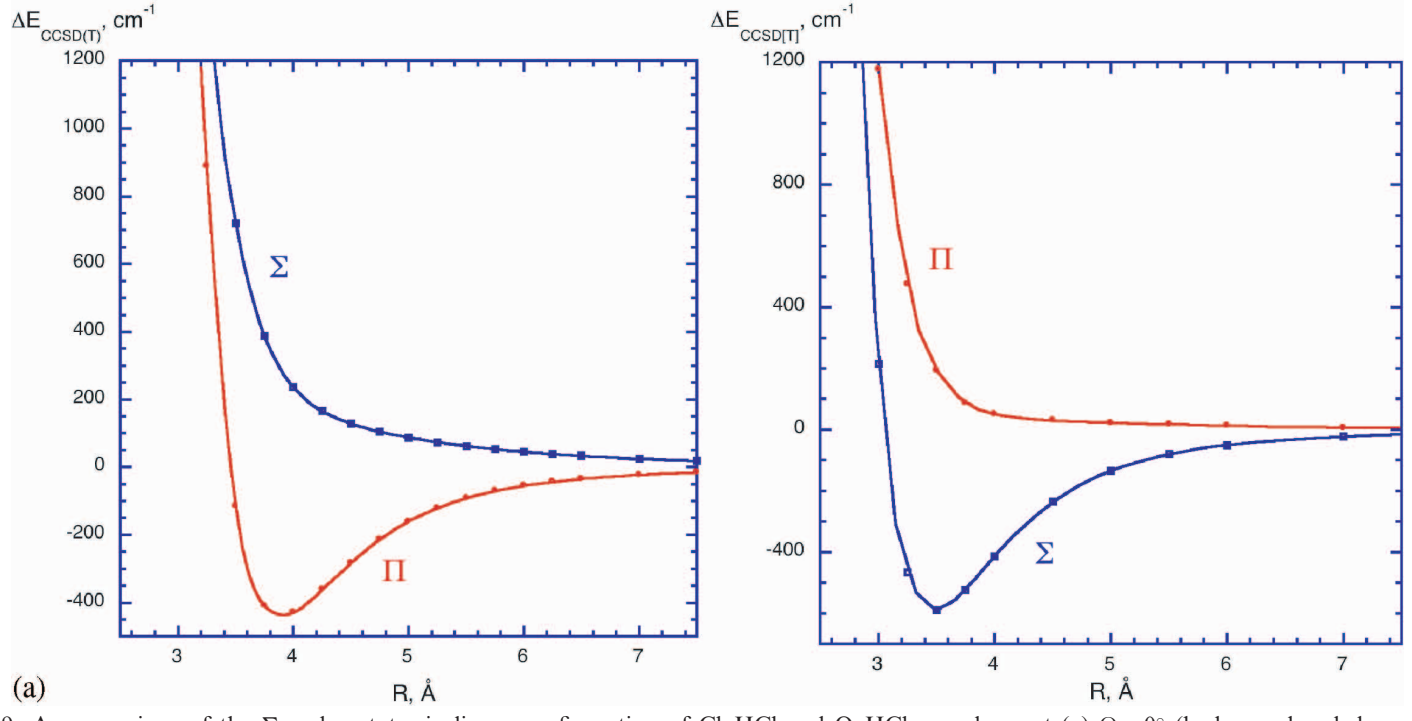

Figure 9. A comparison of the Σ and π states in linear configuration of Cl–HCl and O–HCl complexes at (a) $\Theta = 0^\circ$ (hydrogen-bonded geometries) and (b) $\Theta = 180^\circ$ (non-hydrogen-bonded geometries).

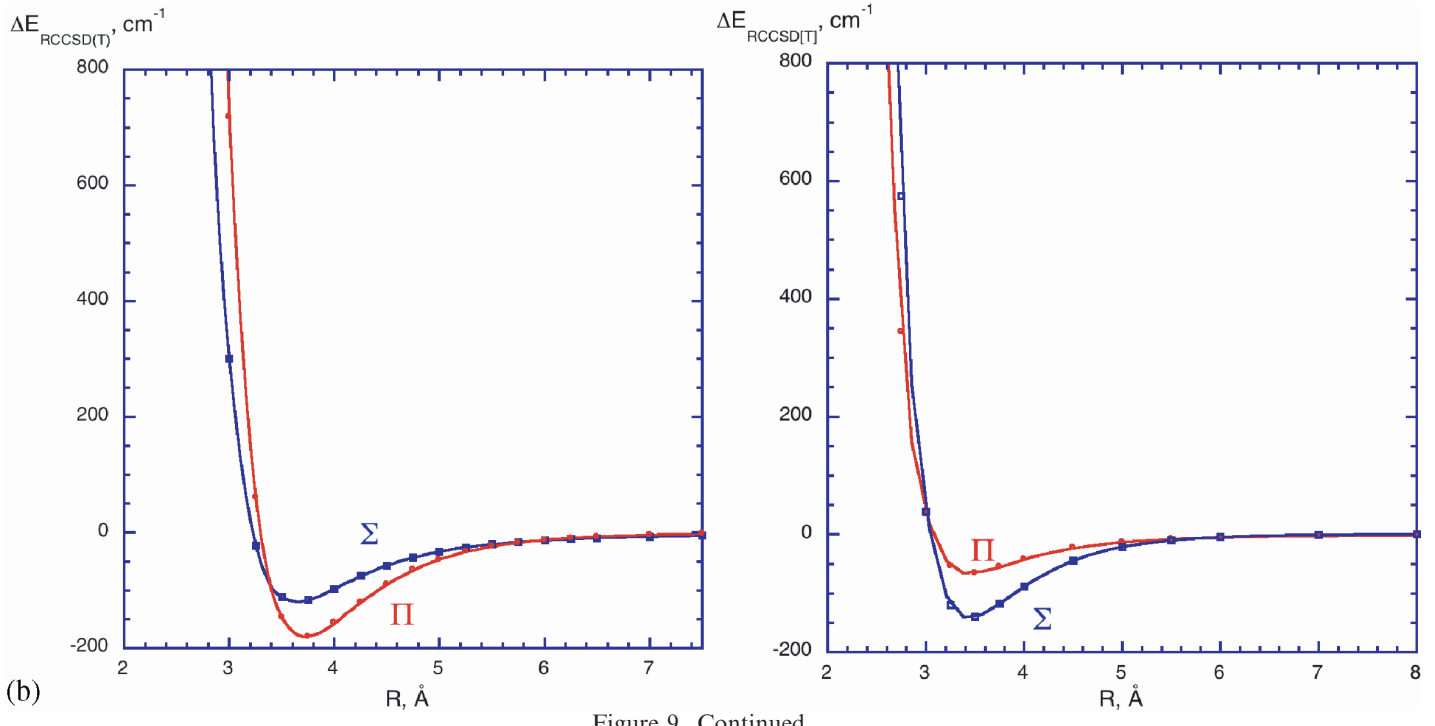

Figure 9. Continued.

Table 3. $O(^3P) + HCl$ minimum characteristics for the three adiabatic ($1A''$, $2A''$, A') and three diabatic (V_{11}, V_{22}, $A' = V_{33}$) PESs from *ab initio* calculations [67]; energy values in cm^{-1}.

PES	Θ (°)	R (Å)	△CCSD(T)/avqz	CCSD(T)/avqz + 332211 bf	MRCI/CBS*
$1A''$	0	3.50	589	595	538
$2A''$	180	3.45	65	74	
$A' = V_{33}$	100	3.50	589	590	
V_{11}	0	3.50	589	595	
	180	3.45	144	151	
V_{22}	90	3.25	203		

*From Ref. [66].

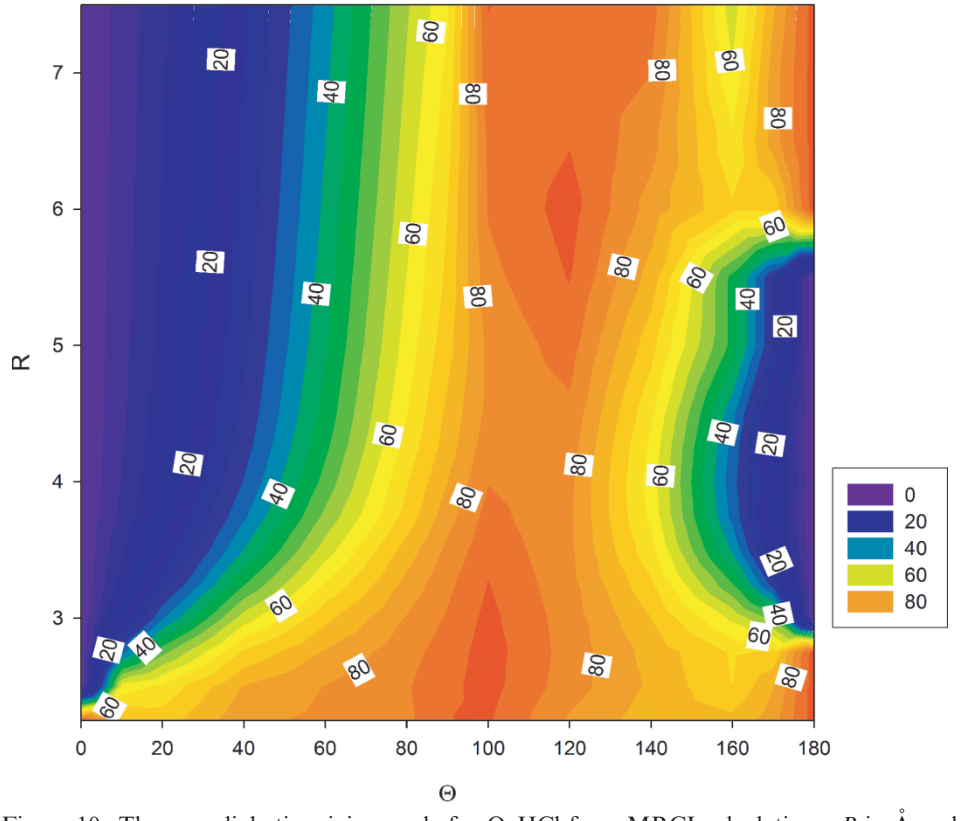

Figure 10. The nonadiabatic mixing angle for O–HCl from MRCI calculations; R in Å and Θ in degrees.

mentioned that the region $R > 6$ Å, $\Theta = 180°$ of the coupled surfaces, that is past the more distant conical intersection, is very difficult to handle computationally. The two surfaces are only a few cm^{-1} apart and the MRCI approach cannot be reliably applied in the context of the CP procedure. We found that this region can be reliably described using the diabatic multipole expanded dipole–quadrupole + quadrupole–quadrupole interaction. The diagonalization of this representation yields the two electrostatic adiabats.

3.3.5. *$X(^2P) + H_2$ ($X = F$, Cl, Br). Description of PESs: Model CC-M*

The interactions between a ^{2}P halogen and the H_2 molecule cause a much weaker splitting of the PESs, hence the application of a single-reference CCSD(T) was not justified, except for the high symmetry C_{2v} and C_{8v} geometries, and the calculations of MRCI interaction potentials (in the context of the CP correction) were very difficult. The approach that we found very accurate and reliable was a model approach (called CC-M) that involved evaluating the *diabats* by applying CCSD(T) calculations for the C_{2v} and C_{8v} high-symmetry geometries and the Legendre-polynomial interpolation for the lower symmetry C_s orientations. For example, the first two diabatic potentials V_{11} and V_{22} were represented as

$$\begin{aligned} V_{11}(R, r, \Theta) &= V_{A_1}^{CCSD(T)}(R, r) \sin^2 \Theta + V_{\Sigma}^{CCSD(T)}(R, r) \cos^2 \Theta \\ V_{22}(R, r, \Theta) &= V_{B_2}^{CCSD(T)}(R, r) \sin^2 \Theta + V_{\Pi}^{CCSD(T)}(R, r) \cos^2 \Theta \end{aligned} \tag{6}$$

In the third diabat V_{33} the $V_{B_1}^{CCSD(T)}$ potential was connected with $V_{\Pi}^{CCSD(T)}$ in a similar fashion. The off-diagonal term V_{12} was obtained from the MRCI calculations of the 1A′ and 2A′ states and the mixing angle γ_{BF}

$$V_{12} = \left(V_{1A'}^{MRCI} - V_{2A'}^{MRCI}\right) \cos \gamma_{BF} \sin \gamma_{BF} \tag{7}$$

In this instance the CP correction of the MRCI potentials was not necessary (see Section 3). The adiabatic surfaces were then obtained by a diagonalization of this representation. This model approach was applied to $Cl(^2P) + H_2$ [54], $Br(^2P) + H_2$ [55] and $F(^2P) + H_2$ [53]. For all three systems the model adiabatic PESs were corrected for the effects of SO-coupling [23] (see Section 2). The CC-M model approach, modified so as to account for higher symmetries, was also applied to the evaluation of the three diabatic surfaces for the entrance-channel complex in a very important reaction, $Cl(^2P) + CH_4$ [68].

The sets of three adiabatic and four diabatic PESs for $Cl(^2P) + H_2$, $Br(^2P) + H_2$ and $F(^2P) + H_2$ are remarkably similar to each other, hence only $Cl(^2P) + H_2$ is shown in figures 11–14. In all three cases the 1A′ (spin-free) adiabats have the minima for the T-shaped structure; the 2A′ surfaces display a double-minimum character (cf. figure 14), and the 1A″ have minima for the linear configuration (cf. figure 12 (bottom)). The effects of SO coupling are again quite dramatic (figure 15): the minimum regions become shallower and smoothed-out, in addition to an obvious effect of raising one surface to the halogen's $^2P_{1/2}$ asymptote. We have also incorporated the explicit dependence of the PESs on the intrasystem coordinate r. For the equilibrium r(H–H) in $F + H_2$, the lowest reactive PES already displays a cleavage in the repulsive barrier. Such a feature is absent in both $Cl + H_2$ and Br–H_2. This points to a different type of attack on H_2 by F, compared to Cl and Br. While the small-sized F can act as a wedge in splitting the H–H bond, the larger Cl and Br atoms tend to break the H–H bond by a collinear pull.

Other surfaces for these complexes that are available in the literature are for $F + H_2$ [21], $Cl + H_2$ [22, 69] and $Br + H_2$ [26]. In general, they represent full reactions and all of them were derived using the MRCI technique. The third source of these potential surfaces is the recent work by Aquilanti *et al.*, who proposed the semiempirical entrance-channel PESs for $Cl + H_2$ and $F + H_2$ reactions by fitting to scattering experiments [36]. As the recent bound-state calculations [37, 38] indicate,

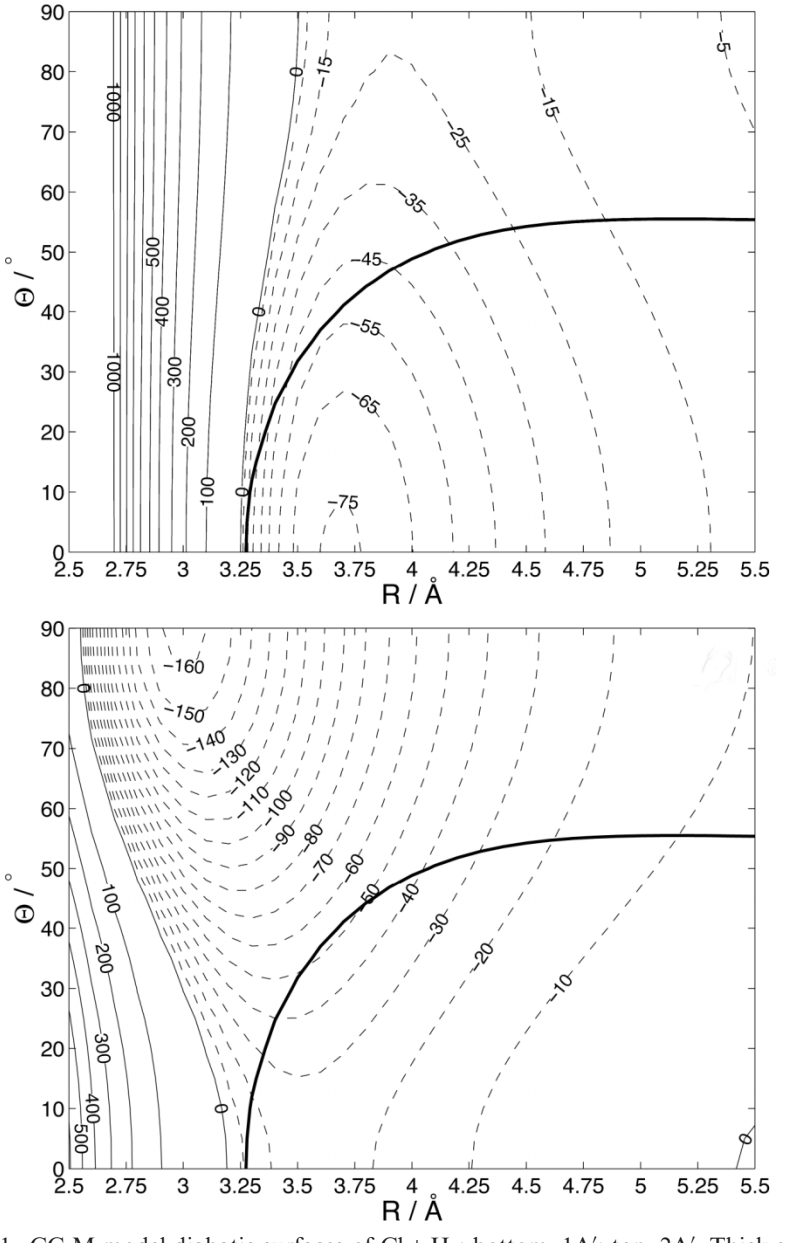

Figure 11. CC-M model diabatic surfaces of $Cl + H_2$: bottom, 1A′; top, 2A′. Thick solid line indicates crossing. Contours are in cm^{-1}.

our PESs led to very similar bound states as these by Aquilanti *et al.* [36], whereas those of Capecchi and Werner [22] led to different results.

The calculations of bound ro-vibrational states for $F + H_2$ reveal interesting details concerning the dynamics of this complex [37]. The complexes of F with *para*-H_2 ($j =$ even) and *ortho*-H_2 ($j =$ odd) are distinctly different. The binding energy D_0 is 14.6 cm^{-1} for the *para*-H_2 complex and 19.3 cm^{-1} for the *ortho*-H_2 complex. In the *para* case the ground-state ($J = 1/2$, parity +) ro-vibrational function slightly favors

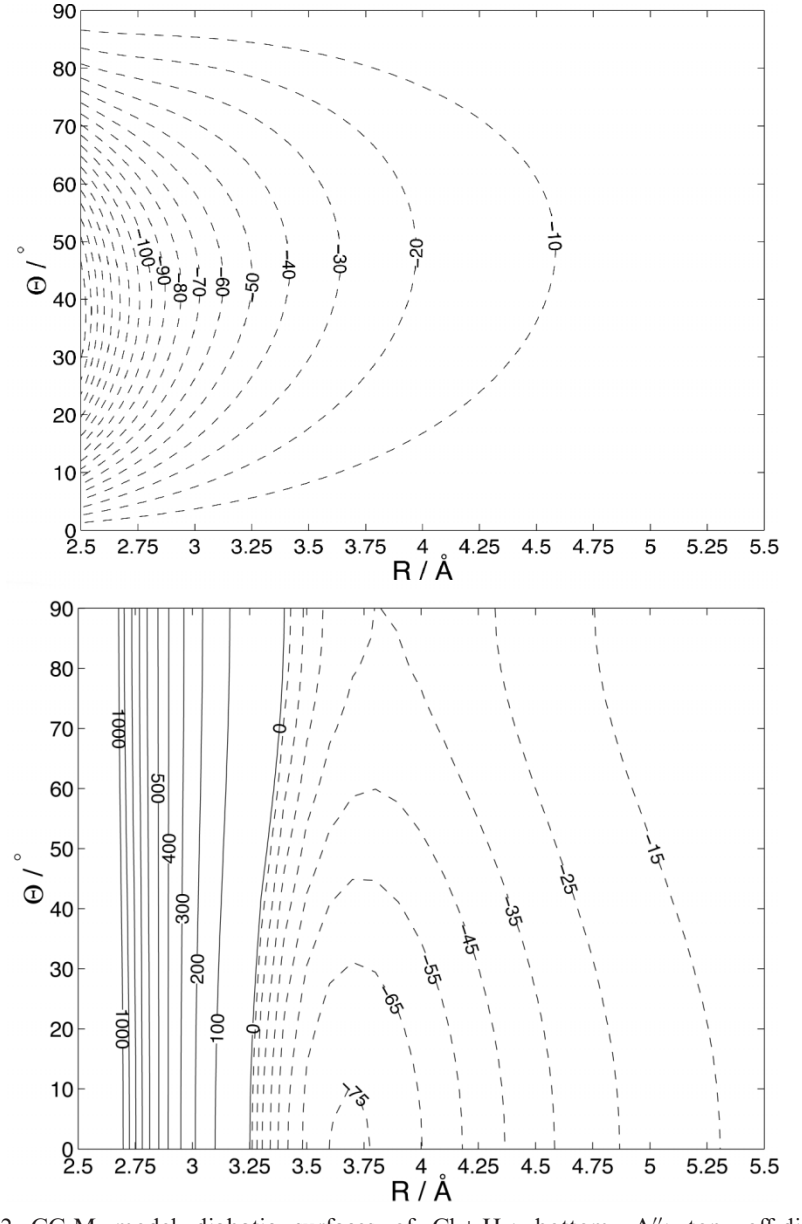

Figure 12. CC-M model diabatic surfaces of $Cl + H_2$: bottom, A″; top, off-diagonal coupling term from MRCI calculations. Contours are in cm^{-1}.

the T-shaped geometry, but the probability density is largely isotropic. By contrast, in the *ortho* case ($J = 1/2$, parity +), the ground state has the ro-vibration function strongly localized at the T-shaped form. This is in line with simple intuition that the *para*-H_2 is isotropic because of its null angular momentum, whereas the *ortho*-H_2 displays anisotropy. The same methodology applied to our CC-M model surfaces for Cl–H_2 and Br–H_2 led to similar ordering of the ground states: Cl + *para*-H_2 $D_0 = 36.8\,cm^{-1}$ vs. Cl + *ortho*-H_2 $D_0 = 43.21\,cm^{-1}$; Br + *para*-H_2 $D_0 = 39.93\,cm^{-1}$ vs. Br + *ortho*-H_2 $D_0 = 45.5\,cm^{-1}$ [38].

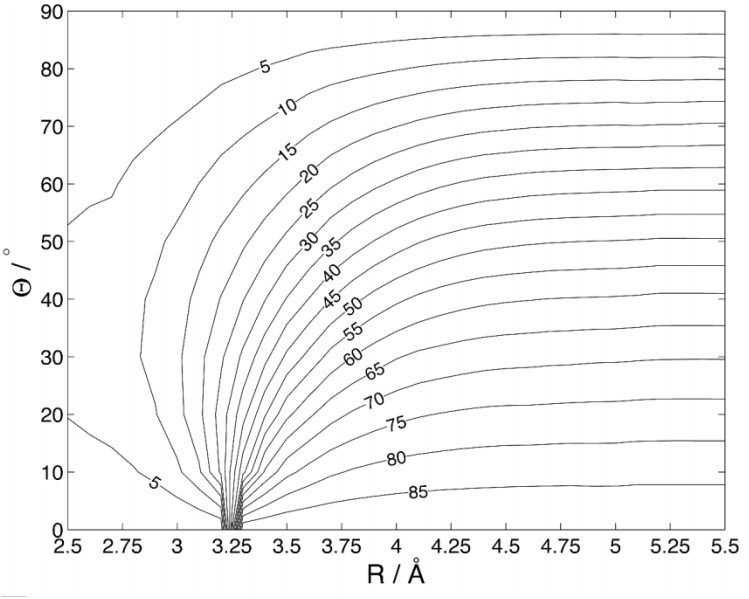

Figure 13. Contour plot of nonadiabatic mixing angle for Cl–H_2. The conical intersection at *ca.* $R = 3.25$ Å of the Σ ($R < 3.25$ Å) and π ($R > 3.25$ Å) states.

The $Cl + H_2$ reaction has been the subject of an interesting experimental controversy that Alexander *et al.* described as "one of the major currently unresolved problems in the dynamics of elementary chemical reactions" [7, 8]. The experimental studies by Liu *et al.* [70] suggested that, in violation of the Born–Oppenheimer approximation, the excited spin–orbit state of Cl ($^2P_{1/2}$) is more reactive towards H_2 than the ground state ($^2P_{3/2}$). This result, if true, would have to involve a purely nonadiabatic process. Neither the state-of-the-art multisurface quantum-scattering calculations by Alexander *et al.* [7] nor the new experimental studies by Balucani and colleagues [71, 72] found such an abnormality. Recently, Alexander *et al.* [73] examined all sources of nonadiabatic behavior in this reaction and found that the nonadiabaticity is determined by the relative magnitudes of the SO coupling constant and the splitting between the reactive and nonreactive PESs in the region of the van der Waals minimum. Again the crucial role of this pre-reactive region has been emphasized.

4. Conclusions

The recent results of *ab initio* calculations on open-shell atom–molecule pre-reactive complexes have been presented. The list of complexes includes X(^{2}P)–HX and X(^{2}P)–H_2 (X = F, Cl, Br) and O(^{3}P)–HCl. It seems that the electrostatic interaction between the nonspherical open-shell atom (halogen or oxygen) and a closed shell molecule with a nonvanishing dipole or quadrupole moment is a key factor in determining the character of these complexes, including the shape of the coupled surfaces and the magnitude of coupling between them. In X(^{2}P), O(^{3}P)–HX complexes this interaction is sizable, causing a large splitting between the surfaces and the rich topology of the PESs. Minima as deep as 800 cm^{-1} (e.g. for Br–HBr) are obtained on the lowest adiabatic surface. The F–HF complex differs from

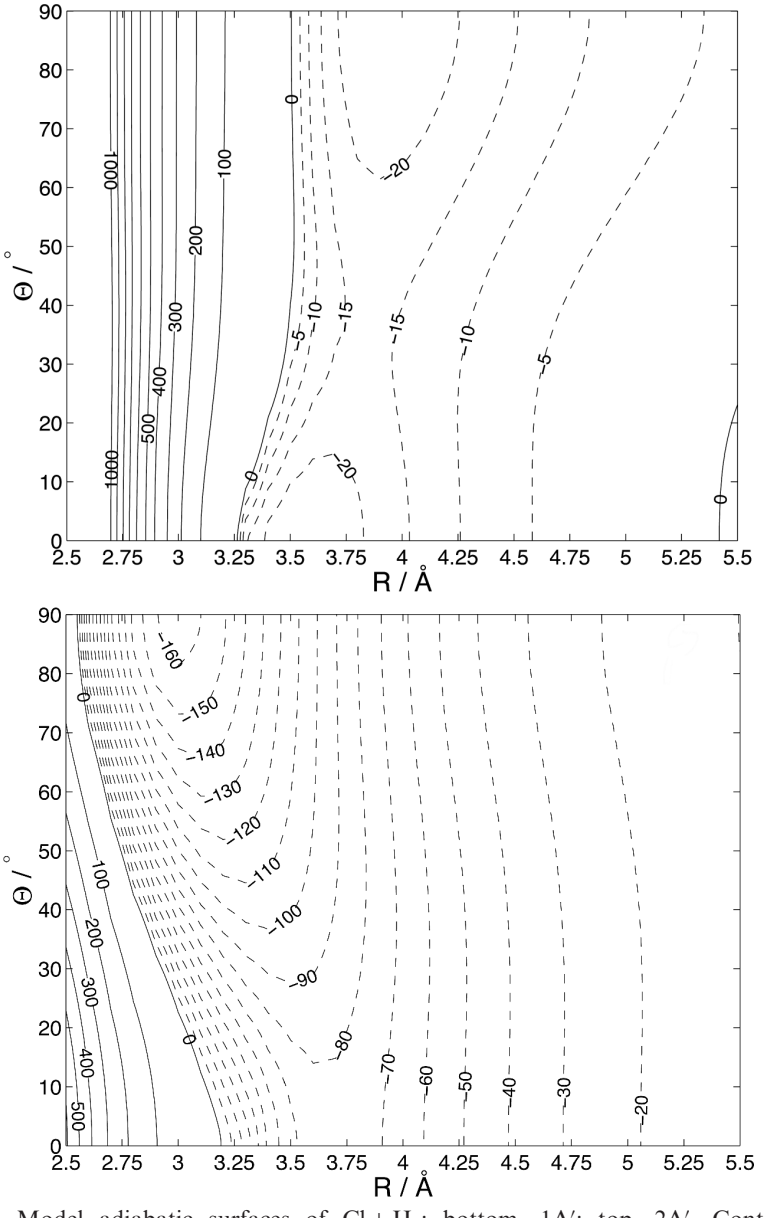

Figure 14. Model adiabatic surfaces of $Cl + H_2$: bottom, 1A′; top, 2A′. Contours are in cm^{-1}.

Cl–HCl and Br–HBr in that it has the linear H-bonded configuration as the global minimum on the lowest adiabatic surface, while the remaining ones have the T-shaped minima. The $X–H_2$ complexes have much weaker splittings and their surfaces are much flatter. The adiabatic PESs of all three complexes have a very similar topology.

The spin-free picture of these complexes does not hold upon inclusion of the SO coupling, which is sizable in halogens and increases from F to Br. The SO coupling washes out the T-shaped minimum and the linear configuration becomes most

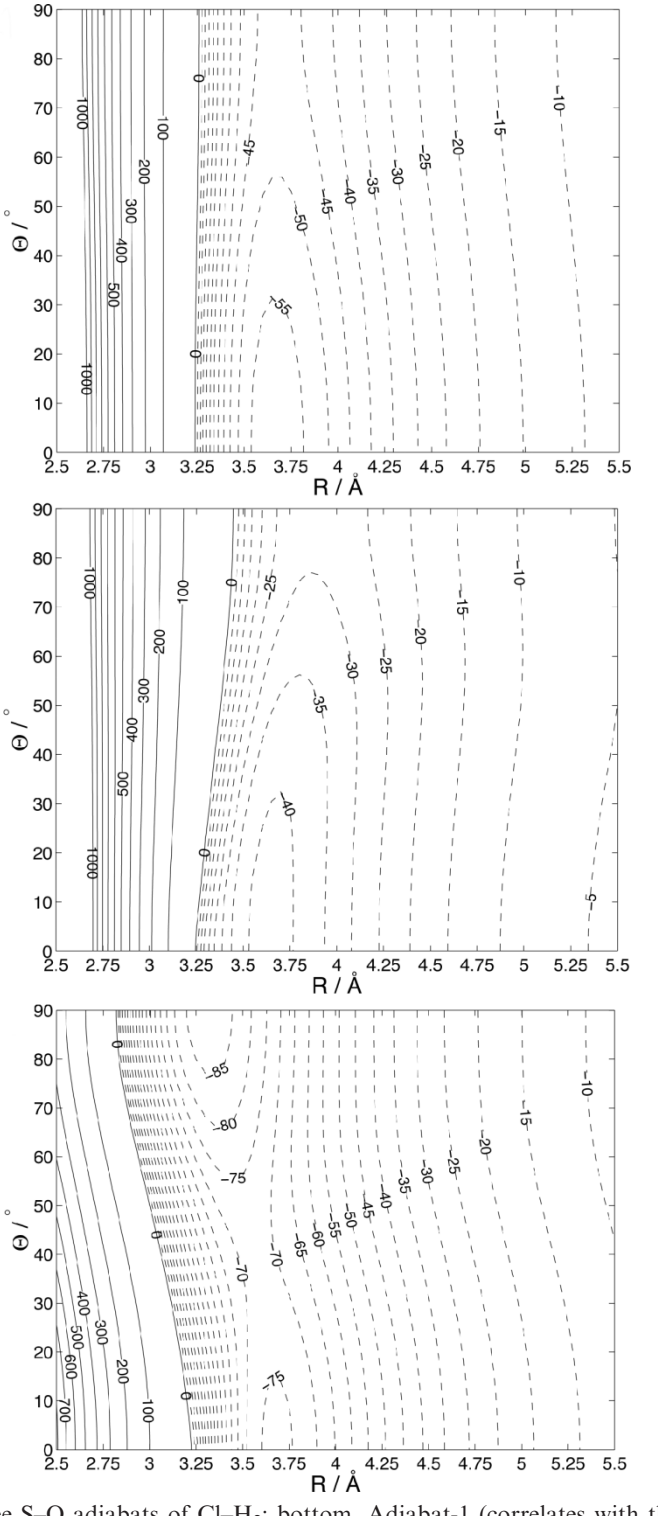

Figure 15. Three S–O adiabats of Cl–H_2: bottom, Adiabat-1 (correlates with the $^2P_{3/2}$ state of Cl); middle, Adiabat-2 (correlates with the $^2P_{3/2}$ state of Cl); top, Adiabat-3 (correlates with the $^2P_{1/2}$ state of Cl).

stable. In the X–H_2 complexes the effect is similar; the global minima become shallower by about one-half.

Examination of the adiabatic-to-diabatic transformation angle is also very instructive. The plots are strikingly similar in Cl + HCl, Br + HBr and O + HCl. They display one conical intersection on the reactive side and one or two on the nonreactive side. The F + HF plot is qualitatively different; there is only one reactive intersection and the angle varies monotonically; a similar shape is also typical of the X + H_2 plots. It seems that these plots, in particular for larger distances, reflect the electrostatic nature of the interactions (which act to orient orbitals in the two coupled states). The plots of the first type occur for interactions with sizable dipole–quadrupole interactions, whereas the plots of the second type occur in the interactions with weaker dipole–quadrupole interaction or quadrupole–quadrupole interaction only. How accurate the electrostatic picture of the mixing angle is, remains to be seen. This issue is important for both practical (modeling) and fundamental reasons (understanding its origins). Some 10 years ago, Dubernet and Hutson [4] predicted that effects due to a breakdown of the Born–Oppenheimer approximation in X + HX would be important. The *ab initio* results fully confirm these predictions.

Our computational strategy for the X–HX complexes involved CCSD(T) calculations of the adiabats and MRCI calculations for the mixing angle. In the X + H_2 complexes a model approach was applied that consisted of obtaining the diabatic surfaces by CCSD(T) calculations for the high-symmetry geometries and interpolation of the intermediate, lower symmetry geometries. MRCI was used to calculate the off-diagonal coupling potentials. The adiabatic potentials were obtained by a diagonalization of this diabatic representation. This strategy was predicated on the specific character of the electrostatic interaction in the case of the hydrogen molecule; that is, small in magnitude and only slightly anisotropic. Similar to the X + HX complexes, after allowing for the SO coupling, the T-shaped minimum became half as deep as in the nonrelativistic case. The bound-state calculations [37] showed that the ground state for the *para*-H_2 involves an almost isotropic rotation of H_2, whereas the ground state of *ortho*-H_2 involves a strongly localized motion around the T-shaped geometry. Similar calculations for Cl + H_2 and Br + H_2 predicted a basically analogous dynamic behavior with the deeper minima capable of supporting a larger number of bound states [38].

Calculated PES manifolds and ro-vibration dynamics are yet to be tested against spectroscopic observations. Experiments with great potential for future insights into the X + HX complexes involve spectroscopy in He nanodroplets by Miller's group [19]. In recent photoelectron spectroscopy experiments by Neumark's group [17], photodetachment from the negative ion $Cl^- + H_2$ was shown to allow access to the entrance channel of Cl + H_2. Low-resolution photoelectron spectra featured transitions to the $^2P_{3/2}$ and $^2P_{1/2}$ states of the Cl + H_2 neutral complexes. A theoretical analysis by Buchachenko *et al.* [74] shows that the first transition can be predicted qualitatively on the basis of the *ab initio* bound states in the ionic and neutral complexes. More work, both experimental and theoretical, is needed to obtain quantitative information and to shed more light on the controversy involving high reactivity of the upper spin–orbit state. As pointed out by Tully [75]: "unanswered questions remain even for these simple and intensively studied systems."

Acknowledgments

This work was supported by the National Science Foundation (CHE-0414241). We thank our collaborators, Joanna Rode, Alexei Buchachenko and Roman Krems, for contributing unpublished results, stimulating discussions and continuous encouragement.

References

[1] Aquilanti, V., Liuti, G., Pirani, F., and Vecchiocattivi, F., 1989, *J. Chem. Soc., Faraday Trans.*, 2 **85**, 955.
[2] Aquilanti, V., and Grossi, G., 1980, *J. Chem. Phys.*, **73**, 1165.
[3] Dubernet, M. L., Flower, D., and Hutson, J. M., 1991, *J. Chem. Phys.*, **94**, 7602.
[4] Dubernet, M. L., and Hutson, J. M., 1994, *J. Chem. Phys.*, **101**, 1939.
[5] Skouteris, D., Manolopoulos, D. E., Bian, W., Werner, H.-J., Lai, L.-H., and Liu, K., 1999, *Science*, **286**, 1713.
[6] Xie, T., Wang, D., Bowman, J. M., and Manolopoulos, D. E., 2002, *J. Chem. Phys.*, **116**, 7461.
[7] Alexander, M. H., Capecchi, G., and Werner, H.-J., 2002, *Science*, **296**, 715.
[8] Manolopoulos, D. E., 2002, *Science*, **296**, 664.
[9] Heaven, M. C., 1993, *J. Phys. Chem.*, **97**, 8567.
[10] Heaven, M. C., 1992, *Annu. Rev. Phys. Chem.*, **43**, 283.
[11] Berry, M. T., Loomis, R. A., Giancarlo, L. C., and Lester, M. I., 1992, *J. Chem. Phys.*, **96**, 7890.
[12] Liu, K., Kolessov, A., Partin, J. W., Benzel, I., and Wittig, C., 1999, *Chem. Phys. Lett.*, **299**, 374.
[13] Zare, R. N., 1998, *Science*, **279**, 1875.
[14] Polanyi, J. C., 1972, *Acc. Chem. Res.*, **5**, 161.
[15] Anderson, D. T., Schwartz, R. L., Todd, M. W., and Lester, M. I., 1998, *J. Chem. Phys.*, **109**, 3461.
[16] Manolopoulos, D. E., Stark, K., Werner, H.-J., Arnold, D. W., Bradforth, S. E., and Neumark, D. M., 1993, *Science* **262**, 1852; Hartke, B., and Werner, H. J., 1997, *Chem. Phys. Lett.*, **280**, 430.
[17] Ferguson, M. J., Meloni, G., Gomez, H., and Neumark, D. M., 2002, *J. Chem. Phys.*, **117**, 8181.
[18] Che, D.-C., Hashinokuchi, M., Shimizu, Y., Ohoyama, H., and Kasai, T., 2001, *Phys. Chem. Chem. Phys.*, **3**, 4979.
[19] Kuepper, J., and Miller, R. E. (in press).
[20] Bauschlicher, C. W., Jr, Langhoff, S. R., Lee, T. J., and Taylor, P. R., 1989, *J. Chem. Phys.*, **90**, 4296; Bauschlicher, C. W., and Partridge, H., 1998, *J. Chem. Phys.*, **109**, 4707.
[21] Stark, K., and Werner, H. J., 1996, *J. Chem. Phys.*, **104**, 6515.
[22] Capecchi, G., and Werner, H. J., 2004, *Phys. Chem. Chem. Phys.*, **6**, 4975.
[23] Alexander, M. H., Manolopoulos, D. E., and Werner, H.-J., 2000, *J. Chem. Phys.*, **113**, 11084.
[24] Manolopoulos, D. E., 1997, *J. Chem. Soc. Faraday Trans.*, **93**, 673.
[25] Skodje, R. T., Skouteris, D., Manolopoulos, D. E., Lee, S.-H., Dong, F., and Liu, K., 2000, *Phys. Rev. Lett.*, **85**, 1206.
[26] Kurosaki, Y., and Takayanagi, T., 2003, *J. Chem. Phys.*, **119**, 7838.
[27] Dobbyn, A. J., Connor, J. N. I., Besley, N. A., Knowles, P. J., Schatz, G. C., 1999, *Phys. Chem. Chem. Phys.*, **1**, 957.
[28] Ramachandran, B., and Peterson, K. A., 2003, *J. Chem. Phys.*, **119**, 9590.
[29] Bussery-Honvault, B., Honvault, P., and Launay, J. M., 2001, *J. Chem. Phys.*, **115**, 10701.
[30] Zyubin, A. S., Mebel, A. M., Chao, S. D., and Skodje, R. T., 2001, *J. Chem. Phys.*, **114**, 320.
[31] Whiteley, T. W. J., Dobbyn, A. J., Connor, J. N. L., and Schatz, G. C., 2000, *Phys. Chem. Chem. Phys.*, **2**, 549.

[32] Xie, T., Bowman, J. M., Peterson, K. A., and Ramachandran, B., 2003, *J. Chem. Phys.*, **119**, 9601.
[33] Benarez, L., Aoiz, F. J., Honvault, P., Bussery-Honovault, B., and Launay, J. M., 2003, *J. Chem. Phys.*, **118**, 565.
[34] Althorpe, S. C., and Clary, D. C., 2003, *Annu. Rev. Phys. Chem.*, **54**, 493.
[35] Klos, J., Chalasinski, G., and Szczesniak, M. M., 2002, *J. Chem. Phys.*, **117**, 4709.
[36] Aquilanti, V., Cavalli, S., Pirani, F., Volpi, A., and Cappelletti, D., 2001, *J. Phys. Chem.*, *A*, **105**, 2401.
[37] Zeimen, W. B., Klos, J., Greonenboom, G. C., and van der Avoird, A., 2003, *J. Chem. Phys.*, **118**, 7340.
[38] Klos, J., Zeimen, W. B., van der Avoird, A., and Alexander, M. H. (in preparation).
[39] Dubernet, M. L., and Hutson, J. M., 1994, *J. Phys. Chem.*, **98**, 5844.
[40] Chalasinski, G., and Szczesniak, M. M., 1994, *Chem. Rev.*, **94**, 1723; Chalasinski, G., and Szczesniak, M. M., 2000, *Chem. Rev.*, **100**, 4227.
[41] Alexander, M. H., 1998, *J. Chem. Phys.*, **99**, 6014; Alexander, M. H., 1993, *J. Chem. Phys.*, **108**, 4467.
[42] Werner, H. J., and Knowles, P. J., 1988, *J. Chem. Phys.*, **89**, 5803.
[43] Boys, S. F., and Bernardi, F., 1970, *Mol. Phys.*, **19**, 553.
[44] Klos, J. A., Chalasinski, G., Szczesniak, M. M., and Werner, H. J., 2001, *J. Chem. Phys.*, **115**, 3085.
[45] Pittner, J., 2003, *J. Chem. Phys.*, **118**, 10876; Li, X., and Paldus, J., 2003, *J. Chem. Phys.*, **119**, 5320; Mahapatra, U. S., Datta, B., and Mukherjee, D., 1999, *J. Chem. Phys.*, **110**, 6171.
[46] Tobita, M., Perera, S. A., Musial, M., Bartlett, R., Noojien, M., and Lee, J. S., 2003, *J. Chem. Phys.*, **119**, 10713.
[47] Baer, M., 1975, *Chem. Phys. Lett.*, **35**, 112.
[48] Rebentrost, F., and Lester, W. A., 1975, *J. Chem. Phys.,* **63**, 3737; 1976, *J. Chem. Phys.*, **64**, 3879.
[49] Zeimen, W. B., Klos, J., Groenenboom, G. C., and van der Avoird, A., 2003, *J. Phys. Chem.*, **107**, 5110.
[50] Medved, M., Fowler, P. W., and Hutson, J. M., 2000, *Mol. Phys.*, **98**, 453.
[51] Szalay, P. G., and Gauss, J., 2000, *J. Chem. Phys.*, **112**, 4027.
[52] Klos, J. A., Chalasinski, G., Szczesniak, M. M., and Werner, H. J., 2001, *J. Chem. Phys.*, **115**, 3085.
[53] Klos, J., Chalasinski, G., and Szczesniak, M. M., 2002, *Int. J. Quantum Chem.*, **90**, 1038.
[54] Klos, J., Chalasinski, G., and Szczesniak, M. M., 2002, *J. Chem. Phys.*, **117**, 4709.
[55] Klos, J., Chalasinski, G., and Szczesniak, M. M., 2002, *J. Phys. Chem.*, *A*, **106**, 7362.
[56] Burcl, R., Chalasinski, G., Bukowski, R., and Szczesniak, M. M., 1995, *J. Chem. Phys.*, **103**, 1498.
[57] Meuwly, M., and Hutson, J. M., 2000, *J. Chem. Phys.*, **112**, 592.
[58] Meuwly, M., and Hutson, J. M., 2000, *Phys. Chem. Chem. Phys.*, **2**, 441.
[59] Meuwly, M., and Hutson, J. M., 2003, *J. Chem. Phys.*, **119**, 8873.
[60] Bitterova, M., and Biskupic, S., 1999, *Chem. Phys. Lett.*, **299**, 145.
[61] Klos, J., Chalasinski, G., and Szczesniak, M. M. (in press).
[62] Schatz, G. C., McCabe, P., and Connor, J. N. L., 1998, *Faraday Discuss.*, **110**, 139.
[63] Yarkony, D. R., 1998, *Acc. Chem. Res.*, **31**, 511; Hoffman, B. C., and Yarkony, D. R., 2000, *J. Chem. Phys.*, **113**, 10091; Yarkony, D. R., 2001, *J. Phys. Chem.*, *A*, **105**, 6277.
[64] Maiti, B., and Schatz, G. C., 2003, *J. Chem. Phys.*, **119**, 12360; Hoffman, M. R., and Schatz, G. C., 2000, *J. Chem. Phys.*, **113**, 9456.
[65] Chalasinski, G., Szczesniak, M. M., and B. Kukawska-Tarnawska, 1991, *J. Chem. Phys.*, **94**, 6677.
[66] Ramachandran, B., and Peterson, K. A., 2003, *J. Chem. Phys.*, **119**, 9590.
[67] Rode, J. E., Klos, J., Szczesniak, M. M., and Chalasinski, G. (in press).
[68] Klos, J., 2002, *Chem. Phys. Lett.*, **359**, 309.

[69] Bian, W., and Werner, H. J., 2000, *J. Chem. Phys.*, **112**, 220.
[70] Dong, F., Lee, S.-H., and Liu, K., 2001, *J. Chem. Phys.*, **115**, 1197; Liu, K., 2001, *Annu. Rev. Phys. Chem.*, **52**, 139.
[71] Balucani, N., Scouteris, D., Cartechini, L., Capozza, G., Segoloni, E., Casavecchia, P., Alexander, M. H., Capecchi, G., and Werner, H.-J., 2003, *Phys. Rev. Lett.*, **91**, 013201.
[72] Balucani, N., Scouteris, D., Capozza, G., Segoloni, E., Casavecchia, P., Alexander, M. H., Capecchi, G., and Werner, H.-J., 2004, *Phys. Chem. Chem. Phys.*, **6**, 5007.
[73] Alexander, M. H., Capecchi, G., and Werner, H.-J., 2004, *Faraday Discuss.*, **127**, 59.
[74] Buchachenko, A. A., Grinev, T. A., Klos, J., Bieske, E. J., Szczesniak, M. M., and Chalasinski, G., 2003, *J. Chem. Phys.*, **119**, 12931.
[75] Tully, J. C., 2004, *Faraday Discuss.*, **127** 463.